

## ***In vitro* and *in vivo* properties of distinct populations of amniotic fluid mesenchymal progenitor cells**

**Maria G. Roubelakis<sup>a, b, \*, #</sup>, Vasiliki Bitsika<sup>a, b, #</sup>, Dimitra Zagoura<sup>a, b</sup>, Ourania Trohatou<sup>a, b</sup>,  
Kalliopi I. Pappa<sup>b, c</sup>, Manousos Makridakis<sup>d</sup>, Aristidis Antsaklis<sup>c</sup>,  
Antonia Vlahou<sup>d</sup>, Nicholas P. Anagnou<sup>a, b, \*</sup>**

<sup>a</sup>Cell and Gene Therapy Laboratory, Centre of Basic Research, Biomedical Research Foundation, Academy of Athens (BRFAA), Athens, Greece

<sup>b</sup>Laboratory of Biology, University of Athens School of Medicine, Athens, Greece

<sup>c</sup>First Department of Obstetrics and Gynecology, University of Athens School of Medicine, Athens, Greece

<sup>d</sup>Biotechnology Laboratory, Centre of Basic Research, Biomedical Research Foundation, Academy of Athens (BRFAA), Athens, Greece

Received: April 20, 2010; Accepted: August 31, 2010

### **Abstract**

Human mesenchymal progenitor cells (MPCs) are considered to be of great promise for use in tissue repair and regenerative medicine. MPCs represent multipotent adherent cells, able to give rise to multiple mesenchymal lineages such as osteoblasts, adipocytes or chondrocytes. Recently, we identified and characterized human second trimester amniotic fluid (AF) as a novel source of MPCs. Herein, we found that early colonies of AF-MPCs consisted of two morphologically distinct adherent cell types, termed as spindle-shaped (SS) and round-shaped (RS). A detailed analysis of these two populations showed that SS-AF-MPCs expressed CD90 antigen in a higher level and exhibited a greater proliferation and differentiation potential. To characterize better, the molecular identity of these two populations, we have generated a comparative proteomic map of SS-AF-MPCs and RS-AF-MPCs, identifying 25 differentially expressed proteins and 10 proteins uniquely expressed in RS-AF-MPCs. Furthermore, SS-AF-MPCs exhibited significantly higher migration ability on extracellular matrices, such as fibronectin and laminin *in vitro*, compared to RS-AF-MPCs and thus we further evaluated SS-AF-MPCs for potential use as therapeutic tools *in vivo*. Therefore, we tested whether GFP-lentiviral transduced SS-AF-MPCs retained their stem cell identity, proliferation and differentiation potential. GFP-SS-AF-MPCs were then successfully delivered into immunosuppressed mice, distributed in different tissues and survived longterm *in vivo*. In summary, these results demonstrated that AF-MPCs consisted of at least two different MPC populations. In addition, SS-AF-MPCs, isolated based on their colony morphology and CD90 expression, represented the only MPC population that can be expanded easily in culture and used as an efficient tool for future *in vivo* therapeutic applications.

**Keywords:** amniotic fluid • MPCs • migration • proteomic analysis • *in vivo* properties

<sup>#</sup>Joint first authors.

\*Correspondence to: Nicholas P. ANAGNOU, M.D., Ph.D.,  
Professor of Biology and Head of Laboratory of Biology  
University of Athens School of Medicine, Athens 115 27, Greece and  
Group Leader, Laboratory of Cell and Gene Therapy  
Foundation for Biomedical Research of the Academy of Athens (IIBEAA),  
Athens 115 27, Greece  
Tel.: +30-210-746-2341; +30-210-746-2356; +30-210-6597-013  
Fax: +30-210-746-2412  
E-mail: anagnou@med.uoa.gr  
<http://www.bioacademy.gr/lab/lab.php?lb=36>

and  
Maria G. ROUBELAKIS, Ph.D.  
University of Athens School of Medicine,  
Athens 115 27, Greece and  
Foundation for Biomedical Research  
of the Academy of Athens (IIBEAA),  
Athens 115 27, Greece  
Tel.: +30-210-6597-013  
Fax: +30-210-6597-545  
E-mail: mrroubelaki@bioacademy.gr  
<http://www.bioacademy.gr/lab/lab.php?lb=36>

# Introduction

Adult bone marrow (BM) mesenchymal progenitors cells (MPCs) or mesenchymal stem cells (MSCs), initially described as precursors of fibroblasts or stromal cells, can be isolated taking advantage of their adhesive properties and can be further expanded in culture. Previous studies demonstrated that MPC populations derived from BM are heterogeneous and contain at least two morphologically distinct subpopulations of cells: (a) spindle-shaped (SS), rapidly self-renewing MPCs and (b) flattened-shaped, slowly self-renewing MPCs [1–4]. More interestingly, this subset of SS MPCs is able to preferentially engraft in mice; thus, they appear more promising tools for clinical applications [5]. Similarly, SS and flattened-shaped MPCs were also isolated from umbilical cord blood (UCB) at clonal level [6], with SS subpopulation exhibiting high expression levels of CD90, whereas the flattened was negative for the same antigen [6].

Recently, our group and others [7–9] have isolated MPCs from an alternative source, the second trimester amniotic fluid (AF), which can be obtained during routine amniocentesis without any ethical concerns [7, 10–12]. We characterized these cells based on their phenotype, multipotency, differentiation potential and on their proteomic profile, constructing a two-dimensional electrophoresis (2-DE) proteomic database of AF-MPCs [7]. Most importantly, AF-MPCs were easily isolated and grew more rapidly under the appropriate culture conditions compared to BM-MPCs [7]. In addition, concurrent studies showed that AF-MPCs, seeded in a scaffold and exposed to osteogenic-inducing medium, were able to form bone after subcutaneous implantation *in vivo*, demonstrating an important role in pre-clinical studies [9].

However, AF-MPCs represent a heterogeneous population composed of multiple categories of adherent cells based on morphological, biochemical and growth characteristics [13–16]. Until now, there is no surface epitope or proposed protocol that can distinguish MPCs *in vitro* and *in vivo* [2]. Therefore, most experiments have been carried out with heterogeneous populations of AF-MPCs [7, 8, 11, 12, 16]. Questions regarding the heterogeneity, the mobilization and homing properties of these cells *in vitro* and *in vivo*, as well as their use as carriers of therapeutic agents are still undetermined.

Therefore, a large number of parameters must be taken under consideration in isolating the rapidly expanding MPCs from AF. First, an important determinant of successful stem cell therapeutic transplantation is the ability of the transplanted cells to home, migrate, efficiently engraft and repair damaged tissues. Various molecules have been shown to regulate these processes in MPCs. Among these are the VLA-5 integrin, which comprises of  $\alpha 5$  (CD49e) and  $\beta 1$  (CD29) subunits and plays key role in migration [7, 8, 11, 17] and the adhesion molecule CD44, which is highly expressed in most of the mesenchymal cell types [18, 19].

Another parameter involves the feasibility of employing genetic modifications on AF-MPCs by introducing therapeutic genes of

interest. For these manipulations, apart from adenoviruses, that have been previously utilized in AF-MPCs [20], lentiviral vectors represent a highly efficient and long-term infection system for transducing stem cells, without the presence of silencing effects during multiple divisions [21–23].

Herein, we have extended our previous findings [7], by isolating and characterizing two different types of AF-MPCs at passage 0 based on their shape, antigen expression levels and functional properties. We named these cells according to their morphology as SS and round-shaped (RS) AF-MPCs. SS-AF-MPCs are characterized by a greater proliferation and multilineage differentiation potential, while they are exhibiting higher levels of CD90 compared to RS-AF-MPCs. Therefore, in the current experiments, we compared their molecular identity, the differentiation capacity and the *in vitro* adhesion properties of both subpopulations. We further analysed the migratory ability, the efficient gene modification and the perspective utilization of SS-AF-MPCs in pre-clinical studies *in vivo*.

## Material and methods

### Isolation and culture of MPCs from human AF

Human AF-MPCs were isolated from 95 AF samples, collected during scheduled amniocentesis between the 15<sup>th</sup> and 18<sup>th</sup> week of gestation [7]. Briefly, second trimester AF samples were obtained, following a written informed consent, approved by the Ethical Committee of the Alexandra Hospital, Athens and the Bioethics Committee of the University of Athens School of Medicine, during scheduled amniocenteses between the 15<sup>th</sup> and 18<sup>th</sup> week of gestation. Amniocentesis was performed under aseptic conditions. Using a 22G needle and under ultrasonographic control, 10–15 ml of AF was aspirated for each sample. The procedure-related spontaneous abortion rate ranges from 0.06% to 0.5% [24, 25]. Samples were collected and 10 ml of each were centrifuged at 1300 rpm for 10 min. The pellet was resuspended in Dulbecco's modified Eagle's medium (DMEM; Sigma-Aldrich, St Louis, MO, USA) supplemented with 20% (v/v) foetal bovine serum (FBS) (Gibco-BRL, Paisley, Scotland, UK), in a 25 cm<sup>2</sup> tissue culture-treated flask and incubated at 37°C in a 5% humidified CO<sub>2</sub> chamber for approximately 20 days, where the first colonies appeared. The medium was then changed every 5 days. The cells were expanded into higher passages and frozen until use.

### Colony forming unit-fibroblast (CFU-F) assay

The CFU-F assay was performed by plating  $1 \times 10^5$  AF cells/well into six-well plates from six randomly selected samples, in the presence of DMEM (Sigma-Aldrich) supplemented with 20% (v/v) FBS (Gibco-BRL). After 18–20 days of culture, CFUs were formed, mechanically selected and sub-cultured separately [26]. The cells from each colony were expanded into higher passages and frozen until use.

## Karyotyping

For karyotyping, RS-AF-MPCs and SS-AF-MPCs from four different samples each, grown in log phase, were harvested and karyotyped using Giemsa stain GTG banding, at passage 5. For SS-AF-MPCs, karyotype was examined at passage 32 as well. Forty metaphase spreads were fully analysed and karyotyped in each case.

## Antibodies and flow cytometry analysis (FACS)

RS-AF-MPCs and SS-AF-MPCs of passage 3–17 were characterized by FACS analysis using CD90, CD166, CD73, CD105, CD44, c-kit, CD34, CD133, CD31, CD29, CD49e, CD45, CD50, CD106, CD11a, CD62P, CD1a, CD13, CD14, CD62E and CD146 [Becton Dickinson (BD), San Jose, CA, USA], SSEA-4 (Abcam, Cambridge, UK), HLA-ABC and HLA-DR (BD) mouse anti-human monoclonal antibodies or appropriate isotype controls (BD). The latter reactions were developed with fluorescein isothiocyanate (FITC)-conjugated goat anti-mouse IgG secondary antibody (DAKO DakoCytomation Ltd., Cambridgeshire, UK). For apoptosis detection, cells were stained with Annexin V-PE (BD) according to manufacturer's instructions. Cells were analysed using a Beckman Coulter Cytomics FC 500 flow cytometer (Beckman Coulter Ltd., Palo Alto, CA, USA). For immunofluorescent staining, anti-collagen type I (Sigma-Aldrich), anti-E-cadherin (Abcam), anti-N-cadherin (Santa Cruz Biotechnology Inc. Santa Cruz, CA, USA) and anti-Vimentin (Thermo Scientific, Fremont, CA, USA) antibodies were used in fixed cells with 4% paraformaldehyde (Sigma-Aldrich). The latter reactions were developed with FITC-conjugated goat anti-mouse IgG (DAKO DakoCytomation Ltd.) or Alexa-488-conjugated goat anti-rabbit (Invitrogen Ltd., Paisley, UK) secondary antibodies, where appropriate. Isotype-matched antibodies were used as negative control. For Oct-4 and Sox-2 nuclear immunofluorescent staining, cells were permeabilized in 0.2% (v/v) Triton-X (Sigma-Aldrich) for 30 min at room temperature after fixation as described above. Cells were then stained with rabbit anti-human Oct-3/4 (Santa Cruz Biotechnology Inc.) or rabbit anti-human Sox-2 (Millipore, CA, USA) antibodies. The latter reactions were developed with Alexa-488-conjugated goat anti-rabbit (Invitrogen Ltd.) secondary antibody. Slides were mounted with Vectashield mounting medium (Vector Laboratories Inc., CA, USA) containing DAPI solution. Cells were visualized and photographed on a Leica CTR-MIC Fluorescent microscope.

## MTS proliferation assay

MTS assay was performed to estimate the proliferation rate of SS-AF-MPCs, RS-AF-MPCs or GFP-SS-AF-MPCs. Cells were plated at a density of  $10^3$  per well in a 96-well plate and cultured for 6–7 days in the presence of DMEM (20% FBS) in five replicates. Appropriate amount of MTS (Promega Ltd, Madison, WI, USA) was added to each well and incubated for 3 hrs. The absorbance was recorded at 490 nm using an ELISA plate reader (ELX 800; Biotek Instruments Inc, VT, USA). The percentage increase of proliferation was calculated using the following formula:  $[(OD_{dayx} - OD_{day0}) / OD_{day0} \times 100]$ . Statistical analysis was performed using the Student's t-test. Three individual samples from each cell type were analysed.

For conditioned medium (CM) preparation, SS-AF-MPCs were cultured until 80% confluency and further allowed to grow in a medium containing 20% FBS for 48 hrs. CM was collected, filtered and stored at  $-20^{\circ}\text{C}$  until use. RS-AF-MPCs were cultured in CM derived from SS-AF-MPCs for 6 days. CM was changed every day.

For temperature proliferation analysis, SS-AF-MPCs at passage 15–20 were cultured for 1 and 6 days in DMEM (20% FBS) at  $37^{\circ}\text{C}$  and  $33^{\circ}\text{C}$ , respectively.

## Transwell migration assay

SS-AF-MPCs (passage 5–15) and RS-AF-MPCs (passage 2–5) were cultured for 48 hrs in DMEM (2% FBS) and then were transferred to the insert of a 8 mm pore size transwell plate, at  $5 \times 10^4 / 100 \mu\text{l}$  density (Corning-Costar, Cambridge, MA, USA). The cells were then allowed to migrate for 16 hrs across the pore membrane, towards human plasma fibronectin (20  $\mu\text{g/ml}$ ; Sigma-Aldrich), laminin I (20  $\mu\text{g/ml}$ ; Sigma-Aldrich) or DMEM (2% FBS). The non-migrated cells were removed from the top of the insert with a cotton swab. The migrated cells were then fixed with 4% paraformaldehyde (Sigma-Aldrich) on the membrane and stained using the Ral Kit (Ral Reactif, Paris, France). For migration blocking experiment, cells were pre-incubated with CD44 (clone 515, BD). Migration was quantified by counting the stained nuclei that passed through the filter. Photographs were taken from a minimum of 10 fields of view ( $20\times$ ) for each membrane and then counted by using Image J software. Three independent experiments were performed each including three replicates. Statistical analysis was performed using the Student's t-test.

## Adhesion assay

SS-AF-MPCs (passage 5–15) and RS-AF-MPCs (passage 2–5) were pre-incubated either with CD44 (clone 515, BD), CD49e (blocking antibody, BD) or IgG1 isotype control (BD) and then transferred to a 24-well plate, coated with fibronectin (Sigma-Aldrich) or hyaluronic acid (Sigma-Aldrich). Non-treated SS- and RS-AF-MPCs were used as positive controls. Cells were let to adhere for 2 hrs and then the supernatant was removed. The adherent cells to the bottom of the well were fixed with 4% (w/v) paraformaldehyde (Sigma-Aldrich), stained using the Ral Kit (Ral Reactif). Photographs were taken from a minimum of 10 fields of view ( $20\times$ ) for each membrane and then counted by using Image J software. Three independent experiments were performed, each including three replicates. Statistical analysis was performed using the Student's t-test.

## RT-PCR procedure

Total RNA was extracted from the cells using the Tri Reagent (Sigma-Aldrich) according to the manufacturer's instructions. The mRNA was reverse transcribed to cDNA using the M-MLV Reverse Transcriptase-RNase H Minus kit (Promega Ltd.).

## Real-time quantitative PCR and semi-quantitative PCR

Real-time quantitative PCR was conducted on an ABI Prism 7700 apparatus [Applied Biosystems (ABI), Foster City, CA, USA]. Each cDNA sample was mixed with specific primer sets and PCR master mix (Applied Biosystems, No. 4312704). TaqMan RT-PCR was used for oct-4, nanog and sox-2 gene expression analysis with primers and conditions designated by Assays on Demand™, Gene Expression Products [ABI Hs00742896\_s1 (oct-4),

1 Hs02387400\_s1 (nanog), Hs01053049\_s1 9 (sox-2), respectively]. Data  
2 were analysed with the ABI Prism 7700 SDS software (ABI). The expres-  
3 sion of oct-4, nanog and sox-2 was normalized to GAPDH internal control  
4 (GAPDH, ABI, No. 433764T), as described by Zannettino *et al.* [27]. The  
5 levels of gene expression were normalized after subtracting the Ct value of  
6 the GAPDH internal control from that of the x (x = oct-4, nanog or sox-2)  
7 Ct value for SS-AF-MPCs and RS-AF-MPCs ( $\Delta Ct = |Ct_x (SS-AF-MPCs \text{ or } RS-AF-MPCs) - Ct_{GAPDH}|$ ). To compare the levels of oct-4, nanog and sox-2  
8 expression between SS-AF-MPCs and RS-AF-MPCs, the  $\Delta\Delta Ct$  value was  
9 determined using the formula ( $\Delta\Delta Ct = \Delta Ct_x(SS-AF-MPCs) - \Delta Ct_x(RS-AF-MPCs)$ ). Then, the relative level of oct-4, nanog and sox-2  
10 expression in SS-AF-MPCs was compared to RS-AF-MPCs by setting the oct-4, nanog and sox-2 expression in  
11 RS-AF-MPCs value to 1 and determining the fold change in expression  
12 against this value using the following formula:  $2^{\Delta\Delta Ct}$ .

13 PCR reaction for albumin was performed using cDNA, primer pairs and  
14 Go Taq<sup>®</sup> Green master mix (Promega Ltd.). The primers used were: F:  
15 5'-AGATGACAACCCAAACCTCCC-3' and R: 5'-CAGCAGCAGCAGAGTAATC-3'.  
16 The semi-quantitative PCR analysis was determined by using the Image J  
17 software after normalization to the  $\beta$ -actin endogenous control (F:  
18 5'-TCTACAATGAGCTGCGTGTG-3' and R: 5'-CAACTAAGTCATAGCCGCC-3').

## 21 Differentiation assays

### 23 Osteogenic differentiation

24 To induce osteogenic differentiation SS-AF-MPCs or RS-AF-MPCs of  
25 passage 5–7 were cultured to 60–70% confluency in osteogenic medium  
26 for 3 weeks, as described previously [7]. The differentiation potential for  
27 osteogenesis was assessed by alkaline phosphatase staining using BCIP/NBT  
28 reagent (Sigma-Aldrich), according to the manufacturer's instructions.

### 30 Adipogenic differentiation

31 SS-AF-MPCs or RS-AF-MPCs of passage 5–13, grown as described above,  
32 were treated with adipogenic medium for 3 weeks, as described previously  
33 [7]. Medium changes were carried out twice weekly. For the determination  
34 of adipogenic differentiation, formation of intracellular lipid droplets was  
35 monitored under microscope and was confirmed by Oil Red O staining  
36 (Sigma-Aldrich).

### 38 Chondrogenic differentiation

39 To induce chondrogenic differentiation, SS-AF-MPCs or RS-AF-MPCs of  
40 passage 5–10, were cultured in high-density pellet mass cultures. Briefly,  
41  $2.5 \times 10^5$  cells were placed into a conical polypropylene tube with 0.5 ml of  
42 defined medium, consisting of DMEM (Sigma-Aldrich) supplemented with  
43 5.33  $\mu$ g/ml linoleic acid (Sigma-Aldrich), insulintransferrin-selenium<sup>+</sup>  
44 (ITS<sup>+</sup>) (Sigma-Aldrich), 1.25 mg/ml bovine serum albumin (Sigma-Aldrich),  
45 10 ng/ml transforming growth factor  $\beta$ 3 (TGF- $\beta$ 3) (Peprotech),  $10^{-7}$ M  
46 dexamethasone (Sigma-Aldrich), 0.17 mM ascorbate acid (Sigma-Aldrich)  
47 and 0.35 mM L-Proline (Sigma-Aldrich). Cells were centrifuged at 2000 rpm  
48 for 5 min and maintained at 37°C for 21 days. Medium was changed twice a  
49 week. After 21 days of pellet mass culture, the pellets were fixed in 10%  
50 formalin (Sigma-Aldrich), paraffin embedded, sectioned and stained with  
51 Alcian Blue (Sigma-Aldrich) and haematoxylin and eosin (Sigma-Aldrich).

### 52 Hepatogenic differentiation

53 For hepatogenic differentiation, SS-AF-MPCs or RS-AF-MPCs of passage  
54 5–13, at  $1.0\text{--}1.3 \times 10^4/\text{cm}^2$  density, were treated with appropriate hepato-  
55 genic medium, as described previously [7]. Hepatogenesis was assessed

after 3 weeks by periodic acid-Schiff (PAS) staining (Sigma-Aldrich),  
measurement of urea concentration (Urea UV Liquid, Technologia Diagnostics,  
Greece) using the Chemwell 2910 autoanalyzer (Awareness Technology  
Inc., Palm City, FL, USA) and determination of albumin expression by  
semi-quantitative PCR.

Osteogenic, adipogenic and PAS hepatogenic differentiation assays  
were quantified by microscopic analyses of 10 fields per image using the  
Image J software.

## Proteomic analysis–mass spectrometry (MS)

Three samples of SS- or RS-AF-MPCs of passage 5–10 were analysed by  
2D-gel electrophoresis in duplicate each, as described before [7]. Protein  
spots were manually excised, tryptic digested and Peptide Mass  
Fingerprinted [7]. Stringent criteria were used for protein identification  
with a maximum allowed mass error of 25 ppm (parts per million) and a  
minimum of five matching peptides [29]. Notably, a high percentage of the  
proteins were identified based on 10 matches. The probability of a false  
identity was usually lower than  $10^{-5}$ . All selected proteins were identified  
and further analysed for their functional properties by the Swiss-Prot  
(<http://expasy.org/sprot/>) and Human Protein Reference Databases  
(<http://www.hprd.org/>). 2DE image analysis was performed by the use of  
the PD-Quest 8.0 (BioRad, Hercules, CA, USA) software package. Protein  
expression was shown as a ratio of the intensity of protein spots in SS-AF-  
MPCs to RS-AF-MPCs or vice versa in ppm. Comparison of the expression  
level of the various protein spots was conducted by the use of Student's  
t-test and Mann-Whitney test. In all cases,  $P < 0.05$  (95% confidence  
levels) was considered statistically significant.

## Western blot

Total proteins of SS-AF-MPCs and RS-AF-MPCs were separated by 10%  
SDS-PAGE and electroblotted to Hybond-ECL NC membrane (Amersham  
Biosciences, Sweden). Protein extracts were derived from a pool of three  
SS-AF-MPCs or RS-AF-MPCs individual samples of different passages,  
respectively. After blocking, membranes were incubated overnight at 4°C  
with the primary antibodies: mouse anti-human CK18 (DakoCytomation),  
mouse anti-human Cathepsin (BD) or mouse anti-human CK19  
(DakoCytomation). Mouse anti-human  $\beta$ -actin antibody (Sigma-Aldrich)  
was used as a control of equal loading. Membranes were then incubated  
with anti-mouse HRP-conjugated secondary antibody (Santa Cruz  
Biotechnology Inc.) and developed by ECL (Perkin-Elmer, MA, USA) detec-  
tion system. Films were scanned and images were analysed using Quantity  
One software (BioRad).

## Lentiviral vector generation, production and transduction of SS-AF-MPCs

The four plasmid expression lentiviral system containing the  
pCCLsin.PPT.hPGK.GFP plasmid [28] was kindly gifted by Prof. L. Naldini  
and used for enhanced GFP expression. Virus was produced by transient  
transfection into 293T cells, as previously described [29], and collected by  
ultracentrifugation using an Ultracentrifuge Discovery 100 Sorvall (Thermo  
Fisher Scientific Inc., Waltham, MA, USA). The concentrated virus was  
resuspended in PBS supplemented with 0.5% BSA (Sigma-Aldrich). The  
lentiviral titres were determined by infection of HT1080 cells with  
serial dilutions of the concentrated viral stock. GFP fluorescent cells were

1 identified by fluorescent microscopy and FACS analysis. Titers ranged from  
2  $5 \times 10^8$  to  $3 \times 10^9$  infectious units (IU)/ml. Approximately,  $5 \times 10^4$  per  
3 well SS-AF-MPCs were seeded in a six-well plate 1 day in advance. Virus  
4 was added in a multiplicity of infection (MOI) of 10–100.

## 6 **In vivo engraftment of GFP-SS-AF-MPCs**

7 NOD-SCID mice were kindly provided by Drs G. Vassilopoulos and E. Siapati  
8 and were housed and maintained at the Animal Facility of the Biomedical  
9 Research Foundation of the Academy of Athens (BRFAA). The procedures for  
10 the care and treatment of animals were performed according to the institu-  
11 tional guidelines, which follow the guidelines of the Association for  
12 Assessment and Accreditation of Laboratory Animal Care (AAALAC) and the  
13 recommendations of the Federation of European Laboratory Animal Science  
14 Associations (FELASA) and approved by the Institutional (BRFAA) Animal  
15 Care and Use Committee. Six to eight weeks old animals ( $n = 8$ ) received  
16 intravenously (i.v.) by tail vein injection  $1 \times 10^6$  GFP-SS-AF-MPCs (passages  
17 15–40). The animals were sacrificed 4 and 10 days later and the tissues were  
18 analysed by immunohistochemistry, FACS and RT-PCR. For the detection of  
19 GFP transgene, genomic DNA was isolated from each organ/tissue collected,  
20 using Proteinase K (Sigma-Aldrich), followed by phenol–chloroform extrac-  
21 tion. RT-PCR analysis was carried out using primers designed on the WPRE  
22 sequence of the lentiviral vector present only in the infused GFP-SS-AF-MPCs  
23 (F: 5'-T T C T C C T C C T T G T A T A A A T C C T G G T T-3' and R: 5'-C G C  
24 C A C G T T G C C T G A C A-3') and SYBR master mix (Roche Applied  
25 Sciences, Indianapolis, IN, USA), according to manufacturer's protocol.

26 Further, to assess SS-AF-MPCs viability in matrigel *in vivo*, NOD/SCID  
27 mice of the same age ( $n = 6$ ) received subcutaneously  $1 \times 10^6$  SS-AF-  
28 MPCs in 200  $\mu$ l of matrigel (Sigma-Aldrich) into the tail base. As negative  
29 control,  $1 \times 10^6$  SS-AF-MPCs in 200  $\mu$ l of PBS were used. The animals  
30 were sacrificed 1 and 10 days later and the matrigel mass was excised and  
31 photographed. Cells were then disassociated by the use of 2% (w/v) colla-  
32 genase (Sigma-Aldrich) for 2 hrs at 37°C and analysed by FACS.

## 33 **Immunohistochemistry**

34 At 4 and 10 days after i.v. injection of GFP-SS-AF-MPCs, animals were sac-  
35 rificed and analysed by immunohistochemistry for GFP or CD90 expres-  
36 sion. Tissues were fixed in 10% formalin (Sigma-Aldrich) and embedded  
37 in paraffin. Non-specific binding was blocked using 10% donkey serum in  
38 PBS. Five-micrometre sections were subsequently incubated with eGFP  
39 (Chemicon, Temecula, CA, USA), CD90 (BD) or appropriate isotype control  
40 antibodies. The reaction was developed with biotinylated goat anti-mouse  
41 secondary antibody (DakoCytomation), followed by ABC-complex-HRP  
42 (DakoCytomation) and DAB (Vector Laboratories Inc.). Slides were coun-  
43 terstained in Gill's haematoxylin (Sigma-Aldrich).

## 44 **Results**

### 45 **Phenotypic characterization of two different** 46 **AF-MPC populations**

47 As reported previously, BM-MSc and UCB-MSc cultures contained  
48 distinct cell types differing at shape and size [4, 6]. In this study, cell  
49

pellets from 95 second trimester AF samples were plated according  
to previous protocols [7] and then plastic adherent cells were  
isolated. Microscopic analysis led to the identification of two mor-  
phological different adherent MPC types in AF, termed as SS (6%,  
five established cell lines) and RS MPCs (94%) (Fig. 1A and B). We  
initially noticed that the percentage of proliferation increase in SS-AF-  
MPCs and RS-AF-MPCs differed during passages 5–7. A more  
detailed analysis revealed that SS-AF-MPCs exhibited high prolifera-  
tive capacity and were passed over 45 passages to date, whereas  
RS-AF-MPCs exhibited a significantly lower proliferative potential  
and reached up to passage 4–7 (Fig. 1C). More importantly, RS-AF-  
MPCs when cultured in CM derived from SS-AF-MPCs exhibited a  
statistically significant increased proliferative potential (Fig. 1C), sug-  
gesting that these cells may require paracrine factors derived from  
the SS-AF-MPCs for expanding. The identification of these two  
different AF populations is of great importance for potential use of  
SS-AF-MPCs in pre-clinical applications and for this reason we  
attempted to investigate their characteristics in more detail.

We first observed that unselected cultures at passage 0–1 con-  
tained a mixture of SS and RS cells [Fig. 1B(i)]. However, at  
two to three passage in 94% of the sample cases of unselected  
cells, the RS cells were more abundant, overtaking the culture  
[Fig. 1B(ii)]. The rest 6% of the samples represented a SS cell  
population [Fig. 1B(iii)] that can be expanded up to 30–50 pas-  
sages to date with normal karyotype [Fig. S1E(i) and (iii)] and high  
proliferation capacity (Fig. 1C). The reason why the SS-AF-MPCs  
were the predominant and the only population at passages 2–3  
onwards in the 6% of the AF samples only, is still undetermined.  
In an attempt to characterize better these two subpopulations, we  
randomly chose six AF samples at passage 0, where a mixture of  
both cell types existed at almost equal frequency. We then  
mechanically isolated 20 individual CFUs, 10 with round and 10  
with SS morphology in total (Fig. 1A). The clonal SS-AF-MPCs and  
RS-AF-MPCs were further expanded *in vitro* and retained their  
morphological characteristics during culture.

The cell surface antigenic characteristics of these two types of  
AF-MPCs were examined by FACS analysis. Both types of  
AF-MPCs were negative for CD34, CD133, CD31, CD45, CD14 and  
HLA-DR. SS-AF-MPCs and RS-AF-MPCs were positive for MSC  
markers CD73, CD105 and CD166, adherent molecules CD29,  
CD44, CD49e and HLA-ABC (Fig. 2). The surface marker profiles  
were consistent with previously reported BM, AF and UCB hetero-  
geneous populations of MSCs [7, 9, 30, 31]. c-kit was expressed  
in similar very low/undetectable levels in both SS-AF-MPCs and  
RS-AF-MPCs populations, whereas CD146 was expressed in  
higher levels in RS-AF-MPCs compared to SS-AF-MPCs (Fig. 2).  
However, we observed that SS-AF-MPCs expressed high levels  
of CD90 [median fluorescent intensity (MFI):  $58.33 \pm 9.68$ ]  
[Fig. 1B(vi)], whereas RS-AF-MPCs showed lower expression  
(MFI:  $7.43 \pm 6.53$ ) [Fig. 1B(v)]. We further noticed that unselected  
cultures at passage 0 exhibited heterogeneous expression for  
CD90, low (MFI  $1.6 \pm 1.45$ ) and high (MFI  $53.4 \pm 4.14$ ), which  
may indicated the initial co-existence of the two different popula-  
tions [Fig. 1B(iv)]. More interestingly, the expression profile of SS-AF-  
MPCs and RS-AF-MPCs remained the same during culture, with

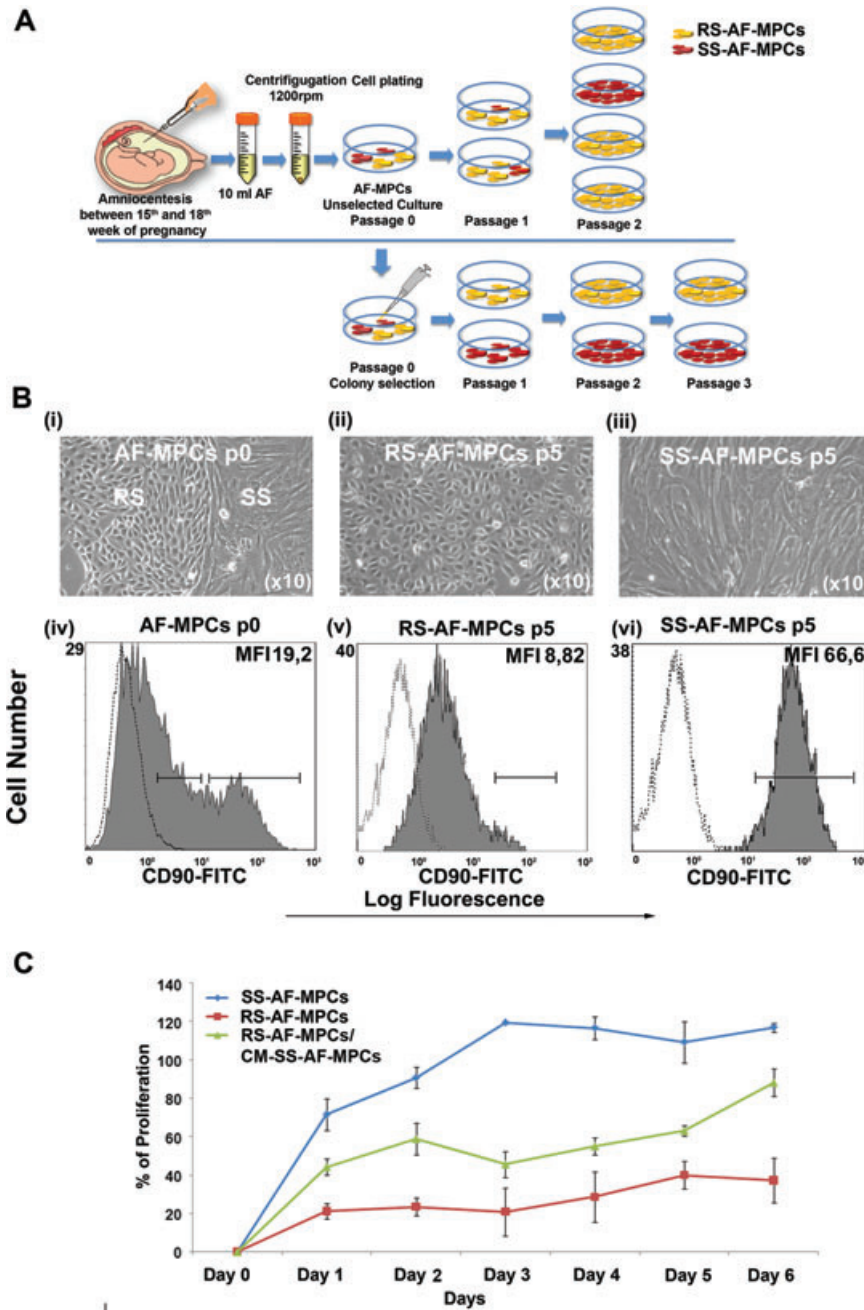


**Fig. 1** Spindle- and round-shaped amniotic fluid mesenchymal progenitor cells. **(A)** Schematic representation of unselected AF-MPCs and mechanically selected colonies in an *in vitro* culture. **(B)** (i) AF-MPCs colonies morphology at p0, (ii) RS-AF-MPCs (p5) and (iii) SS-AF-MPCs (p5) morphology. Representative FACS histograms of (iv) AF-MPCs at p0, gated for CD90 expression (grey filled histograms), prior to analysis with the isotype-matched negative control (open histograms) at p0, (v) homogenous RS-AF-MPC at p5 and (vi) homogenous SS-AF-MPCs at p5 populations, respectively. **(C)** Comparative analysis of the percentage of proliferation of SS-AF-MPCs (blue line), RS-AF-MPCs (red line) and RS-AF-MPCs cultured in CM derived from SS-AF-MPCs (green line), during 6 days of culture by MTS assay. Values are mean  $\pm$  S.D. for three independent samples from each MPC population.

stable CD90 expression for each population, irrelevant to the culture passages and to the *in vitro* MPCs aging (data not shown). Another important observation was that SS-AF-MPCs exhibited high expression levels of CD44 adhesion molecule (MFI:  $58.95 \pm 8.91$ ) compared to RS-AF-MPCs (MFI:  $37.4 \pm 10.46$ ). We additionally examined the expression of MSC markers such as Vimentin and N-cadherin and also the epithelial marker E-cadherin. Both cell types were positive for Vimentin, whereas SS-AF-MPCs expressed E- and N-cadherin in a higher level (Fig. S1A).

### CD90 expression altered according to the proliferation rate of SS-AF-MPCs

In an attempt to examine a potential relation of the enhanced expression levels of CD90 in SS-AF-MPCs with the high proliferation capacity they exhibit, we performed an *in vitro* proliferation assay at different temperature culture conditions. It is known from classical studies that when fibroblast-like cells are cultured at lower temperature (*i.e.* 33°C), they exhibit a lower proliferation rate [32].

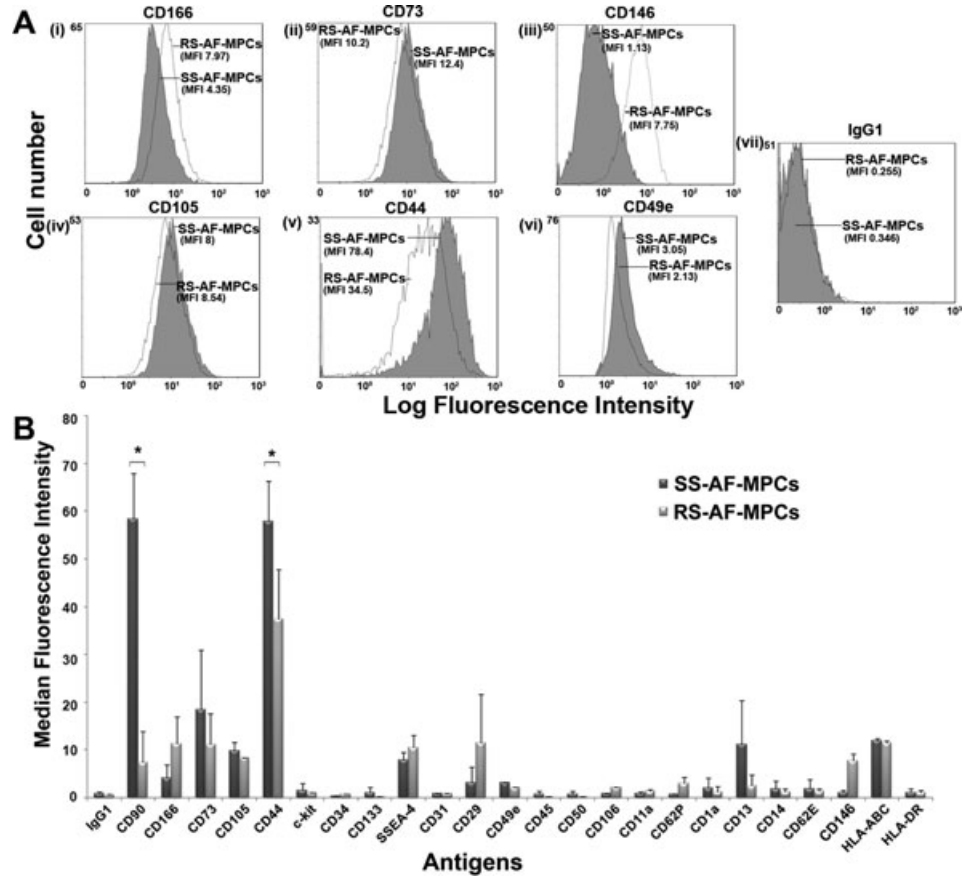


**Fig. 2** Comparison of SS-AF-MPCs and RS-AF-MPCs expression patterns. (A) Representative FACS histograms of SS-AF-MPCs (grey filled histograms) and RS-AF-MPCs (opened histograms) gated for (i) CD166, (ii) CD73, (iii) CD146, (iv) CD105, (v) CD44 and (vi) CD49e markers, prior to analysis with (vii) the isotype-matched negative control. (B) SS- and RS-AF-MPCs analysed for different antigens expression by FACS analysis. The statistics were made on the mean MFI for each antigen. Isotype matched negative controls were used. Values are shown as mean  $\pm$  S.D. for three independent samples from each type. Statistical analysis was performed using the Student's t-test (\* $P < 0.05$ ).

Therefore, we performed proliferation analysis assay for SS-AF-MPCs at 37°C (normal temperature conditions) and 33°C (low temperature conditions), respectively. The proliferation rate of SS-AF-MPCs dramatically decreased when cultured at 33°C for 6 days (Fig. 3A), compared to those cultured at 37°C for the same period. When we examined the expression of mesenchymal-related antigens at these time points, we observed that CD73 and CD105 levels were not altered when SS-AF-MPCs were cultured at 33°C (Fig. 3B). However, CD90 expression was decreased to 60.08%  $\pm$  26.4 for day 1 [Fig. 3B(i)] and 62.09%  $\pm$  3.65 for day 6 [Fig. 3B(ii)], respectively when the proliferation rate of SS-AF-MPCs was reduced because of temperature change. These results showed that CD90 antigen expression might be related to the growth rate of AF-MPCs and may in turn explain the difference of proliferation between the SS-AF-MPCs (CD90<sup>high</sup>) and RS-AF-MPCs (CD90<sup>low</sup>) subpopulations.

**CD44 neutralizing antibody inhibited SS-AF-MPCs migration on fibronectin**

Initially, a transwell migration assay was developed to determine the migration potential of SS-AF-MPCs and RS-AF-MPCs to

fibronectin and laminin. Interestingly, SS-AF-MPCs migrated approximately 7.59- and 7.79-fold faster towards fibronectin and laminin, respectively, than RS-AF-MPCs [Fig. 4A(i)] ( $P < 0.001$ , Student's t-test).

Taking under consideration that CD44 represented an adhesion molecule, binding on fibronectin and was expressed in SS-AF-MPCs in a higher level than RS-AF-MPCs according to FACS analysis (Fig. 2), we further investigated whether this elevated expression has a functional role in migration of SS-AF-MPCs. We therefore performed the same transwell migration assay after pre-incubating SS-AF-MPCs with a neutralizing antibody for CD44. Isotype non-binding antibody (IgG1) was used as a negative control. A significant decrease of 31.05%  $\pm$  12.13 ( $P < 0.05$ , Student's t-test) in migration capacity of SS-AF-MPCs was observed in the presence of CD44 blocking antibody [Fig. 4A(ii)].

**CD44 neutralizing antibody inhibited SS-AF-MPCs and RS-AF-MPCs adhesion on fibronectin and hyalouronic acid**

SS-AF-MPCs and RS-AF-MPCs when tested in an *in vitro* adhesion assay on fibronectin and hyalouronic acid, exhibited similar

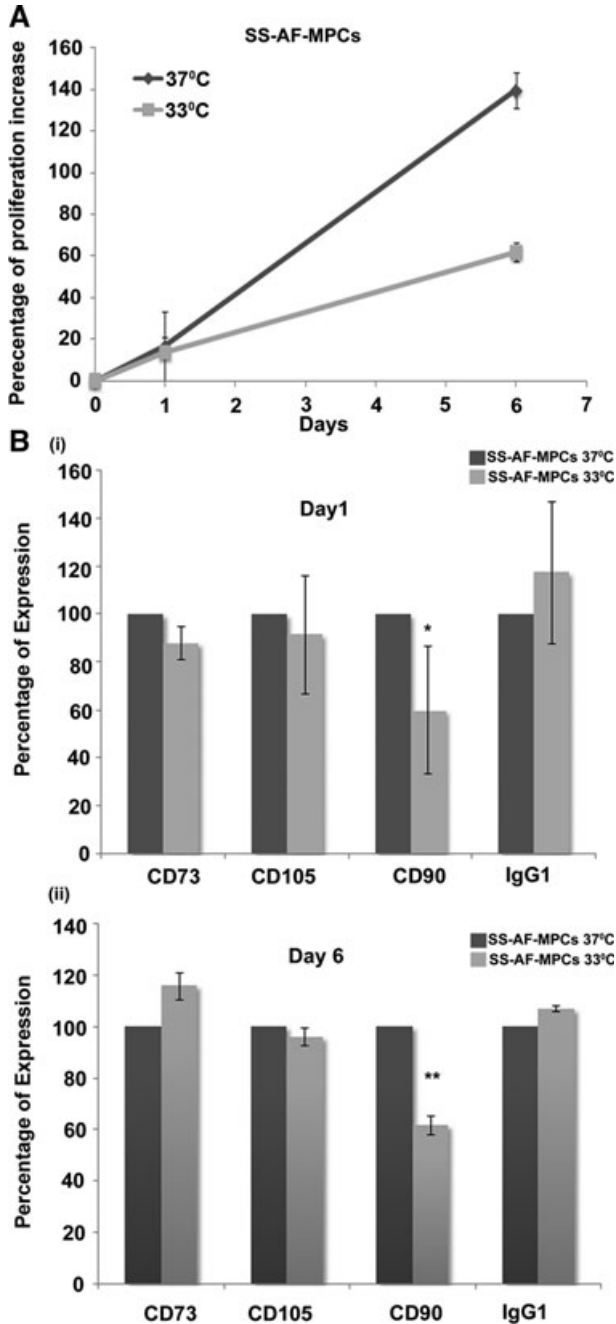


**Fig. 3** CD90 expression alteration according to the proliferation rate of SS-AF-MPCs. **(A)** Comparative analysis of the percentage of proliferation increase of SS-AF-MPCs at 37°C (grey line) and 33°C (light grey line), respectively during 6 days of culture. **(B)** Comparison of the percentage of expression of CD73, CD105 and CD90 (i) at day 1 and (ii) day 6 of culture at 37°C (grey bars) and 33°C (light grey bars) by FACS analysis, respectively. MFI values were normalized for each marker against the level of expression determined at 37°C, which was set to 100%. Values are shown as mean  $\pm$  S.D. for three independent experiments. Statistical analysis was performed using the Student's t-test (\* $P < 0.05$ ; \*\* $P < 0.001$ ).

adhesion capacities on both matrices [Fig. 4B(i-ii)-non-treated cells]. To analyse in detail the role of CD44 adhesion molecule, which binds to fibronectin and also to hyalouronic acid [33], we examined whether CD44 controlled not only the high migration capacity of SS-AF-MPCs as shown before, but also the adhesion of both populations to the respective binding matrices. Blocking of CD44 resulted in lower adhesion of both SS-AF-MPCs and RS-AF-MPCs on fibronectin at approximately 48% ( $P < 0.05$ , Student's t-test) and 31.3% ( $P < 0.05$ , Student's t-test), respectively [Fig. 4B(i)]. However, only SS-AF-MPCs exhibited impaired adhesion on hyaluronic acid in the presence of CD44 blocking antibody, (37.9%,  $P < 0.05$ , Student's t-test). There was no significant effect on cell adhesion using the IgG1 antibody compared to the non treated cells in both matrices [Fig. 4B(i) and (ii)].

### CD49e modulated SS-AF-MPCs and RS-AF-MPCs adhesion properties

Both cell types express the CD49e molecule which binds to fibronectin, as determined by FACS analysis (Fig. 2). For examining the role of CD49e on fibronectin-mediated adhesion, we analysed SS-AF-MPCs and RS-AF-MPCs in an *in vitro* adhesion assay. We observed an approximately 87% ( $P < 0.001$ , Student's t-test) and 68.9% ( $P < 0.001$ , Student's t-test) reduction on adhesion ability of SS-AF-MPCs and RS-AF-MPCs, respectively, in the presence of CD49e blocking antibody, compared to non-treated cells [Fig. 4B(i)].

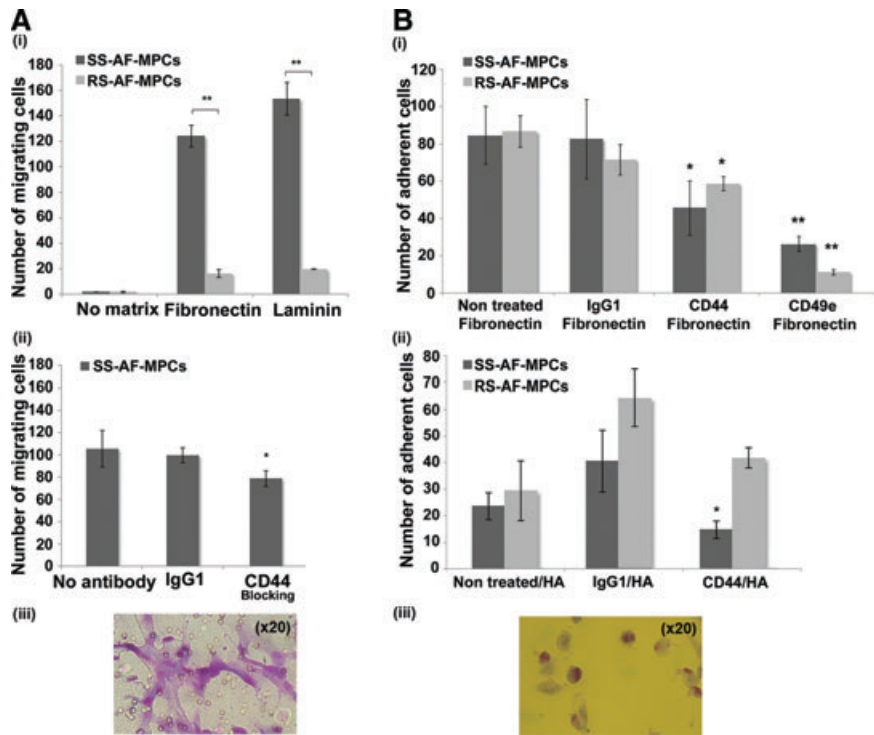
### SS-AF-MPCs expressed oct-4, nanog and sox-2 in higher levels than RS-AF-MPCs

We next examined the expression of the oct-4, sox-2 and nanog transcripts, key markers in embryonic stem cells and responsible for the maintenance of pluripotency of mammalian stem cells *in vivo* and *in vitro*, in SS-AF-MPCs and RS-AF-MPCs of passages 5–7 [34, 35]. Oct-4, nanog and sox-2 exhibited a  $2.6 \pm 1.38$ ,  $10.41 \pm 3.38$  and  $15.18 \pm 3.92$  fold higher expression respectively, in SS-AF-MPCs compared to RS-AF-MPCs, by RT-PCR analysis after normalization to GAPDH endogenous control (Fig. 5A). However, both AF-MPCs types expressed Oct-4 and Sox-2 at protein level, as demonstrated by nuclear immunofluorescent staining (Fig. 5B). In all samples examined, the majority of the cells were positive for Oct-4 and Sox-2.

### SS-AF-MPCs exhibited different differentiation properties compared to RS-AF-MPCs

SS-AF-MPCs and RS-AF-MPCs were cultured under appropriate conditions that induce adipocytes, osteocytes, chondrocytes (mesoderm-derived) and hepatocytes (endoderm-derived), to evaluate their *in vitro* differentiation properties (Fig. 6). Results

**Fig. 4** Migration and adhesion properties of SS-AF-MPCs and RS-AF-MPCs. **(A)** (i) SS-AF-MPCs showed higher motility ( $P < 0.001$ ) on fibronectin and laminin, respectively compared to RS-AF-MPCs. (ii) Number of migrated SS-AF-MPCs to fibronectin in presence of CD44 neutralizing antibody or isotype matched non-specific antibody IgG1. (iii) Representative image (20 $\times$ ) of migrated SS-AF-MPCs fixed and stained using the Ral staining kit on the transwell membrane. **(B)** (i) Number of adherent SS-AF-MPCs and RS-AF-MPCs to fibronectin, treated with CD44, CD49e neutralizing antibodies or isotype matched non-specific antibody IgG1 in comparison to non treated SS-AF-MPCs and RS-AF-MPCs, respectively. (ii) Number of adherent SS-AF-MPCs and RS-AF-MPCs to hyalouronic acid, treated with CD44 neutralizing antibody or isotype matched non-specific antibody IgG1 in comparison to non treated SS-AF-MPCs and RS-AF-MPCs, respectively. (iii) Representative image (20 $\times$ ) of adherent cells fixed and stained using the Ral staining kit on the plastic vessel. Values are shown as mean  $\pm$  S.D. for three independent experiments. Statistical analysis was carried out using the Student's t-test ( $*P < 0.05$ ;  $**P < 0.001$ ).



showed that RS-AF-MPCs exhibited an enhanced adipogenic ( $1.6 \pm 0.4$  fold times increase) [Fig. 6A (iii)] and reduced osteogenic ( $4.6 \pm 1.0$  fold times decrease) [Fig. 6B(iii)] differentiating capacity compared to SS-AF-MPCs, as determined by oil red O and alkaline phosphatase staining and quantified by Image J analysis, respectively. Interestingly enough, under chondrogenic and hepatogenic inducing conditions, RS-AF-MPCs failed to form chondrocytes and hepatocyte-like cells respectively, in contrast to SS-AF-MPCs (Fig. 6C and D). Chondrogenesis, was determined by Alcian Blue staining of pellets (Fig. 6C). Hepatogenesis was verified by PAS staining, where hepatocyte-like cells derived from SS-AF-MPCs exhibited a  $73.07 \pm 5.2$  fold times increase in PAS staining compared to SS-AF-MPCs [Fig. 6D(ii)], urea production ( $46.5 \text{ mg/dl} \pm 10.2$ ) compared to SS-AF-MPCs ( $9.6 \text{ mg/dl} \pm 6.4$ ) [Fig. 6D(iii)] and high albumin expression level ( $12.5 \pm 2.4$  fold expression difference compared to SS-AF-MPCs) [Fig. 6D(iv)].

### Differentially expressed proteins identified in SS-AF-MPCs and RS-AF-MPCs

To further characterize the AF-MPCs subpopulations, proteins differentially expressed in SS-AF-MPCs and RS-AF-MPCs were identified by 2D-gel electrophoresis and MS. Total protein extracts of three different SS-AF-MPCs and RS-AF-MPCs preparations were analysed in duplicate by 2DE in 4–7 pH gradient strips. The derived pattern of resolved protein spots for each cell type was highly consistent and a comparison of the expression levels of the respective

proteins was established using PDQuest 8 software (Fig. 7A and B). Protein spots that were found to be more than 1.5 times fold differentially expressed and at statistically significant levels ( $P < 0.05$  according to Student's t-test and/or Mann-Whitney test) in the two subpopulations, are described in detail in Tables S1 and S2. Specifically, proteins up-regulated in SS-AF-MPCs compared to RS-AF-MPCs included reticulocalbin-3 precursor, collagen  $\alpha 1$  (I) chain precursor, FK506-binding protein 9 precursor, Rho GDP-dissociation inhibitor 1, chloride intracellular channel protein 4, tryptophanyl-tRNA synthetase and heat shock proteins 1 70 kDa and  $\beta 1$ . On the other hand, proteins such as peroxiredoxin-2, 60 kDa heat shock protein, glutathione S-transferase P and annexin A4, were up-regulated in RS-AF-MPCs. Proteins identified only in RS-AF-MPCs included cytoke- ratin 8, 18 and 19, cathepsin B, coactosin-like protein and integrin  $\alpha$ -V protein (Table S3).

Among the proteins overexpressed in SS-AF-MPCs, collagen  $\alpha 1$  (I), a major extracellular matrix molecule responsible for directing the fate of MSCs into osteogenic lineages [36], was the most abundant. This finding may in turn explain the enhanced differentiation potential of SS-AF-MPCs to osteoblastic lineages, as observed in our *in vitro* studies. Proteins facilitating cell migration, such as Rho GDP-dissociation inhibitor 1 [37] and tryptophanyl-tRNA synthetase [38] are expressed in higher levels in SS-AF-MPCs, reflecting their enhanced motility *in vitro*. On the other hand, the high proliferation rate of SS-AF-MPCs might be explained by the presence of proteins such as chloride intracellular channel protein 4, found to promote endothelial cell proliferation and cell survival [39]. Similarly, heat shock protein  $\beta 1$ , exhibiting

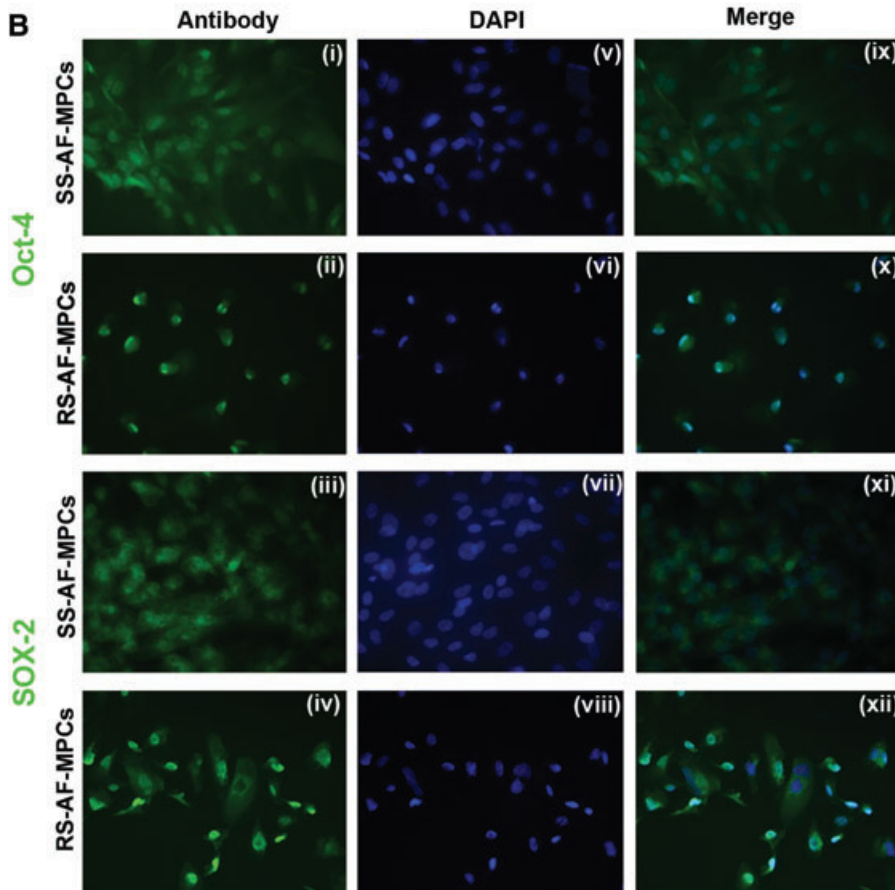
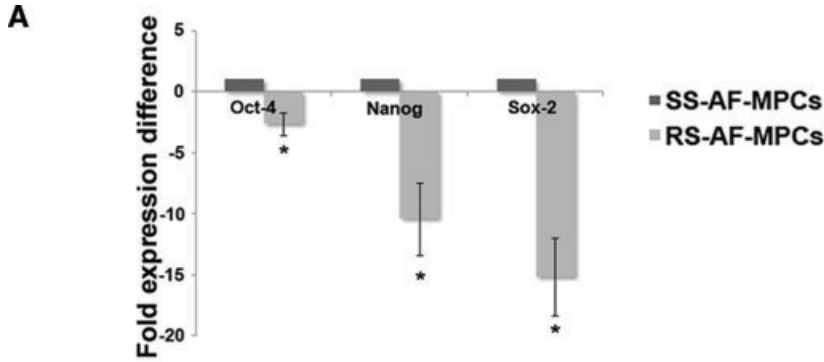


**Fig. 5** Embryonic stem cell marker expression and differentiation potential of SS-AF-MPCs and RS-AF-MPCs. **(A)** Comparative analysis for the expression of oct-4, nanog and sox-2 in three SS-AF-MPCs and RS-AF-MPCs samples, respectively, analysed by RT-PCR. Results were first normalized to human GAPDH positive control and then to SS-AF-MPCs expression levels for each marker, respectively. Statistical analysis was performed using the Student's t-test. **(B)** Immunofluorescent nuclear staining for (i–ii) Oct-4, (iii–iv) Sox-2 and (v–viii) DAPI (ix–xii) of SS-AF-MPCs and RS-AF-MPCs. Merge of DAPI staining and antibody staining. Original magnifications, 40 $\times$ .

an anti-apoptotic role by former studies, was also highly expressed in SS-AF-MPCs [40, 41].

### Confirmation of the differentially expressed proteins CK18, CK19, cathepsin B and collagen $\alpha$ 1 (I)

RS-AF-MPCs exhibited a more complicated protein profile compared to SS-AF-MPCs, including 10 uniquely expressed proteins,

supporting the indication of an earlier developmental stage of the SS population. To verify the 2DE results and confirm the differential expression, cytokeratin 18, cytokeratin 19 and cathepsin B were further analysed by Western blotting. It was demonstrated that bands of 40, 54 and 28 kDa, corresponding to CK19, CK18 and cathepsin B, respectively were only detected in RS-AF-MPCs (Fig. 7C). Furthermore, collagen  $\alpha$ 1 (I) was expressed in higher levels in SS-AF-MPCs than in RS-AF-MPCs again in agreement to the 2DE results (Fig. 7D).

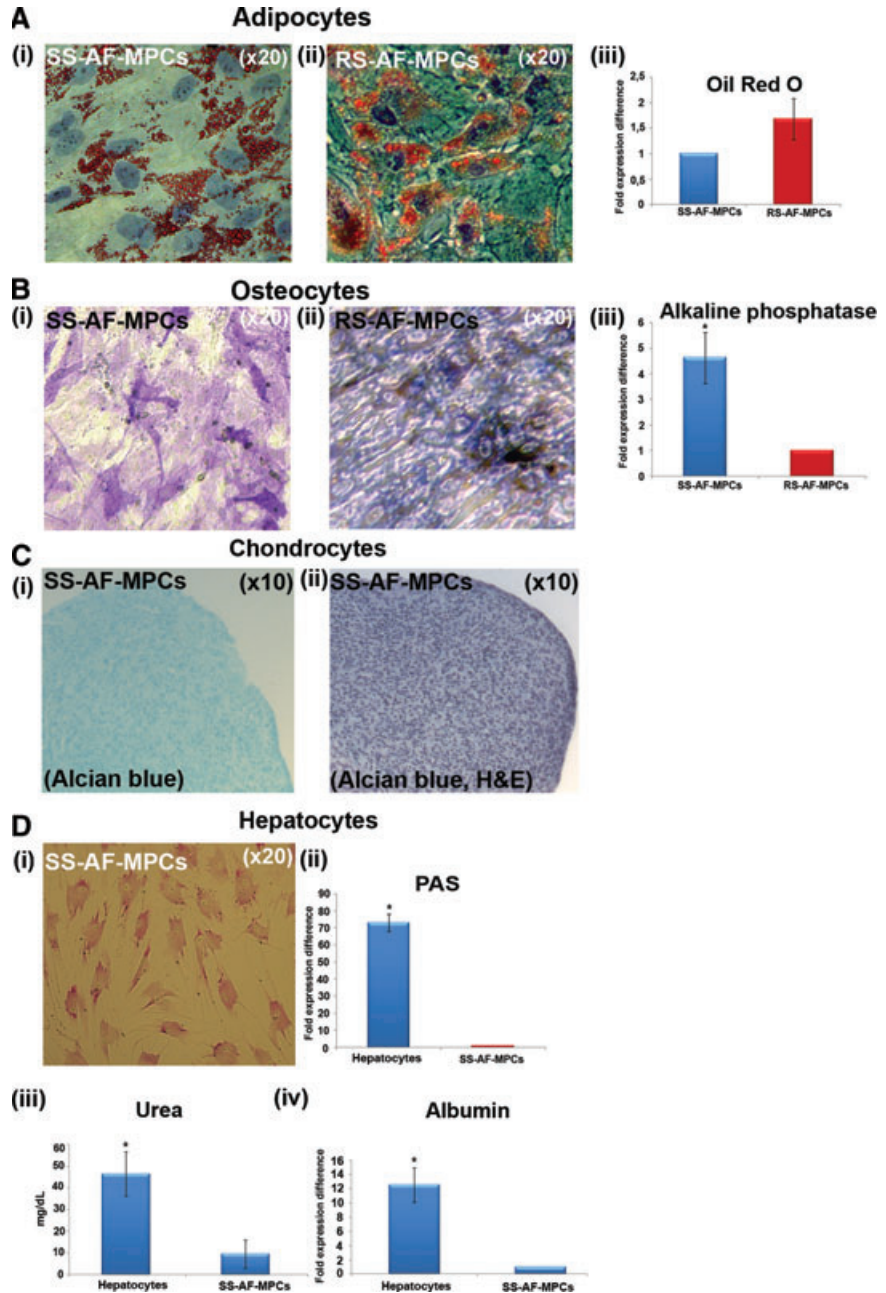


**Fig. 6** (A) Oil Red O staining for adipocyte differentiation for (i) SS-AF-MPCs and (ii) RS-AF-MPCs respectively, followed by (iii) quantitation analysis. (B) Alkaline phosphatase staining for osteocyte differentiation for (i) SS-AF-MPCs and (ii) RS-AF-MPCs respectively, followed by (iii) quantitation analysis. (C) (i) Alcian Blue and (ii) haematoxylin and eosin staining of SS-AF-MPCs, cultured under chondrogenic inducing conditions in pellet mass cultures. (D) PAS staining for hepatocyte differentiation for (i) SS-AF-MPCs induced to hepatocytes. (ii) Quantitation analysis for PAS staining, (iii) determination of the secreted Urea and (iv) albumin expression were shown. Quantitation of the respective differentiation assays was performed by using the Image J analysis software on 10 fields per image. For each sample, four images were taken. For adipogenic and osteogenic differentiation values were normalized in each case against the AF-MPC type with the lower differentiation capacity, which was set to 1, whereas for hepatogenic differentiation, values were normalized in each case against non-induced to differentiation SS-AF-MPCs. Values are mean  $\pm$  S.D. from three samples from each type. Statistical analysis was performed using the Student's t-test,  $P < 0.05$ .

### Lentivirus-mediated gene transfer of AF-MPCs

Taking under consideration the successful, easy and rapid expansion of SS-AF-MPCs in culture, as well as the high passage they reach compared to RS-AF-MPCs, we further investigated whether they can be efficiently transduced with lentiviral vectors for further potential use in *in vivo* therapeutic applications. For this reason, SS-AF-MPCs were transduced with GFP third generation lentivirus [28]. The experimental procedure was focused on three parameters:

first, the efficiency of same passage SS-AF-MPCs transduction by a virus dose-dependent manner; secondly, the efficiency of GFP expression in different passages and thirdly, the long-term maintenance of GFP expression in culture. An increase in fluorescence of GFP positive SS-AF-MPCs was shown, when the cells, at passage 16, were transduced with rising doses of virus, MOI from 10 to 100, as determined by FACS analysis four days post-transduction (Fig. 8A and B). The transduction with an MOI of 60 led to a 98–100% efficiency of infection. A very small percentage of cells

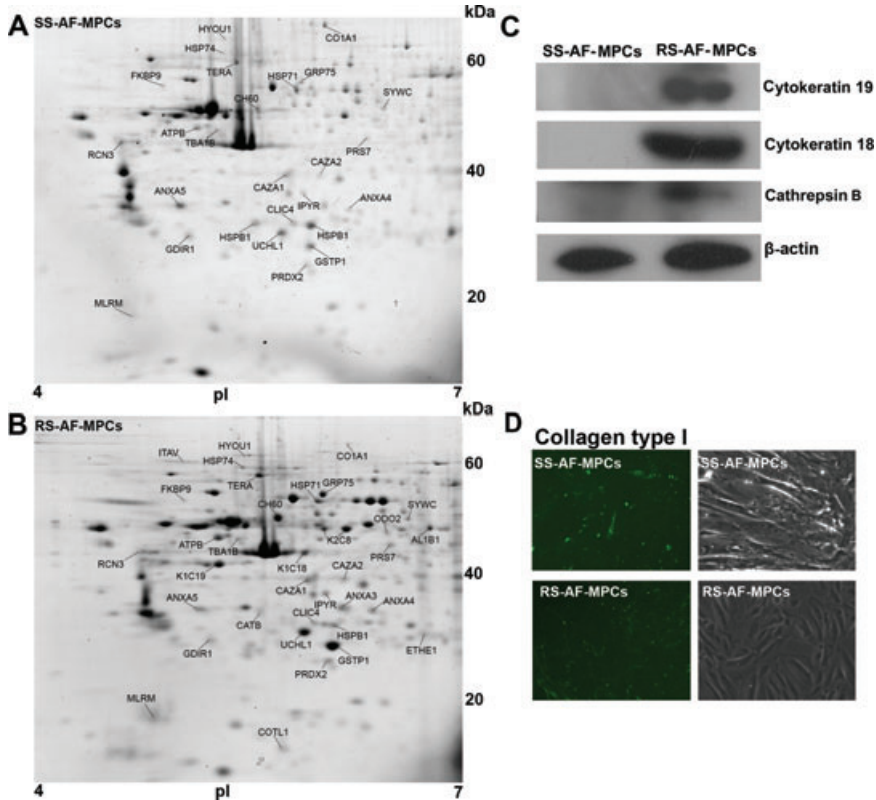


**Fig. 7** Two-dimensional gel electrophoretic analysis of AF-MPCs. **(A)** Representative 2D-gel electrophoresis image of proteins extracted from SS-AF-MPCs and **(B)** RS-AF-MPCs. The differentially and unique expressed protein spots in each population are indicated with their abbreviated names and listed in Tables S1–3, respectively. **(C)** Confirmation of the cytoskeratin 19 and 18 and cathepsin B expression by Western blot analysis with the respective antibodies in cell extracts from SS-AF-MPCs (lanes 1) and RS-AF-MPCs (lanes 2). Protein bands of 40, 54 and 38 kDa corresponding to cytoskeratin 19 and 18 and cathepsin B heavy chain were detected. Immunoblotting for b-actin has been conducted to ensure the comparable loading of proteins in each lane. **(D)** Confirmation of the higher expression of collagen  $\alpha$ 1 (I) protein in SS-AF-MPCs compared to RS-AF-MPCs by immunofluorescent staining.

were positive for Annexin V staining only in virus dosages higher than MOI 60 (Fig. 8C). The expression levels of mesenchymal markers (CD90, CD105 and CD73) in SS-AF-MPCs remained the same after transduction (data not shown).

Furthermore, we performed a different passage expression analysis using SS-AF-MPCs of passages 10–40, transduced with an MOI of 60 (Fig. 8D). Interestingly enough, the passage did not affect the expression of GFP. In addition, the expression of GFP was maintained at the same high levels 4 weeks and 9 months post-transduction (Fig. 8E). By series of freezing and thawing cycles we observed that the expression of GFP remained constant. In addition, GFP-SS-AF-MPCs (MOI 60) exhibited high proliferation capacity (Fig. S1B) and were still capable to differentiate into adipogenic, osteogenic and hepatogenic lineages *in vitro*, as shown in Figure S1C.

### **In vivo** engraftment of left ventricular transduced SS-AF-MPCs

The high proliferation rate of SS-AF-MPCs and the fact that they exhibit normal karyotype at high passages, allowed the use of these cells *in vivo*. RS-AF-MPCs were not efficient in number to be used in *in vivo* experiments.

Thus, we further investigated the *in vivo* survival, migration and engraftment of GFP-SS-AF-MPCs in non-damaged immunosuppressed mice. GFP-SS-AF-MPCs were *i.v.* injected into

NOD/SCID mice and then analyses involving FACS, immunohistochemistry and RT-PCR for the WPRE gene were used, to follow the distribution of donor cells 4 and 10 days post-injection at different tissues (Fig. 9). For immunohistochemistry anti-human CD90 antibody, which does not cross-react with mouse MSCs and tissue (Fig. S1D) was also used. We were able to detect GFP-SS-AF-MPCs at liver, spleen, lung, gut and kidney at these time points. However, similarly to previous studies with MSCs [42], we could not detect SS-AF-MPCs in the BM as confirmed by FACS analysis (data not shown). No tumours were detected even after 3 months post-SS-AF-MPCs transplantation in NOD/SCID animals, which may indicate non-tumorigenic properties of these cells.

Furthermore, we tested the viability of SS-AF-MPCs supported by matrigel and transplanted subcutaneously into the tail bases of NOD/SCID mice. It was demonstrated by fluorescent microscopy and FACS analyses that matrigel succeeded in supporting SS-AF-MPCs engraftment for at least 10 days without losing the GFP expression (Fig. 9D). This finding proved that extracellular components provided by matrigel were needed to improve SS-AF-MPCs survival and engraftment *in vivo*.

## **Discussion**

Recent interest is focused on AF as a valuable source of MPCs [7–9, 11, 12]. Culture of AF-MPCs, as previously reported

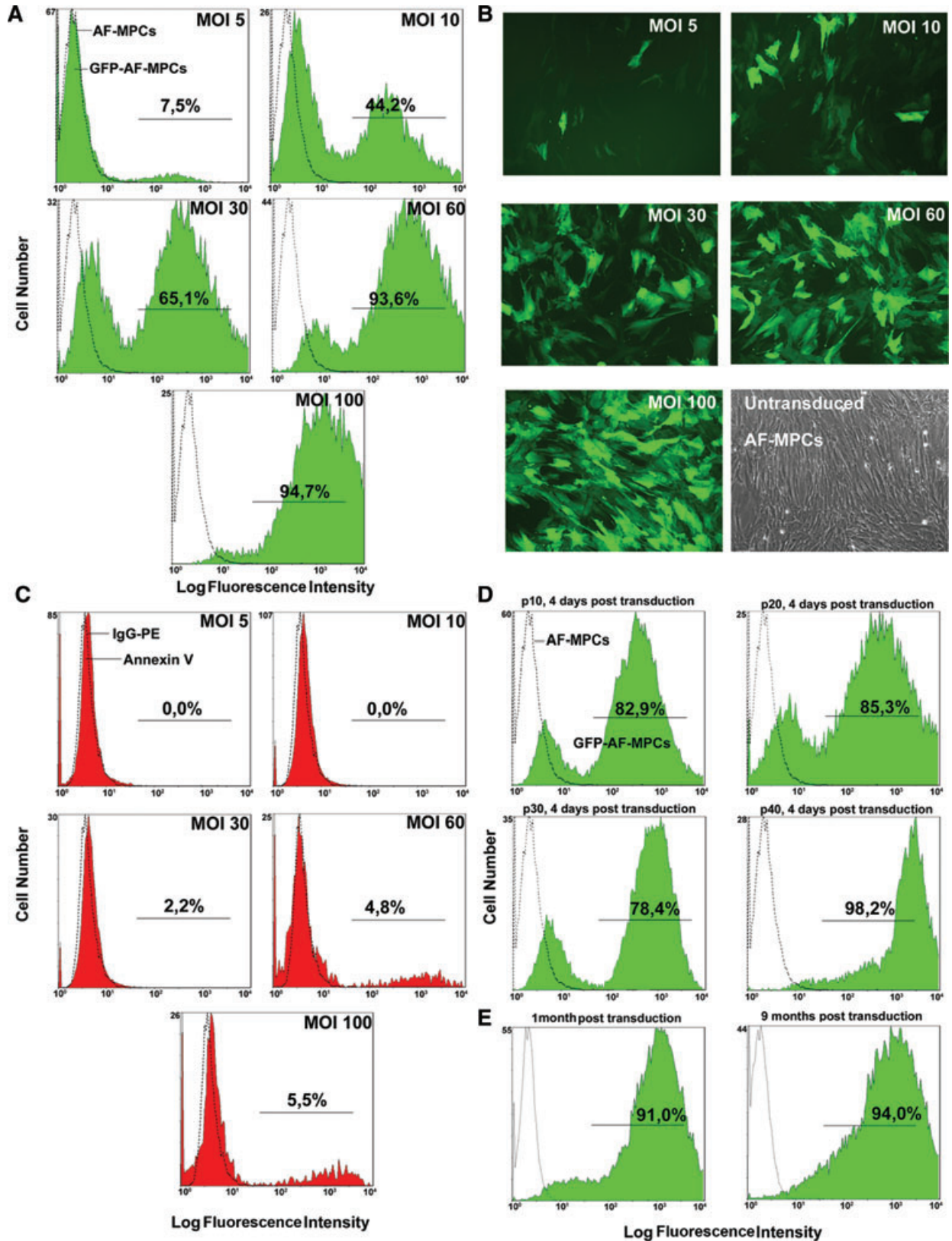




**Fig. 8** Transduction of SS-AF-MPCs with the pCCLsin.PPT.hPGK.GFP lentiviral system. **(A)** Flow cytometric analysis, **(B)** microscopic evaluation (20×) and **(C)** evaluation of apoptosis by Annexin V staining by FACS analysis of SS-AF-MPCs at MOI 5–100 and passage 16 **(D)** GFP efficiency of SS-AF-MPCs determined 4 days post-transduction at passages 10, 20, 30 and 40 by FACS analysis of MOI 60. **(E)** Stability of GFP expression 1 and 9 months post-transduction by FACS analysis at MOI 60.

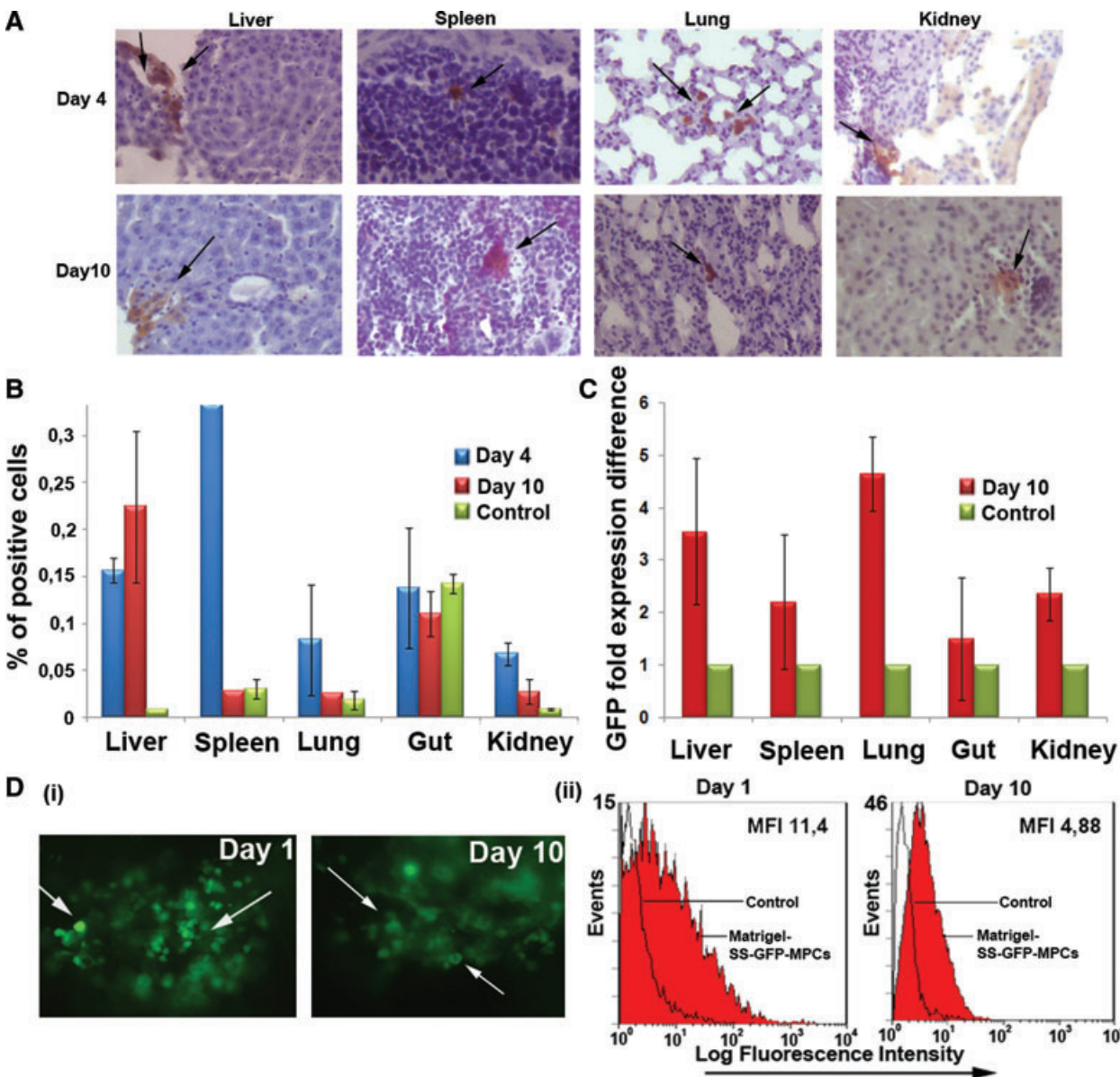


**Fig. 9** *In vivo* engraftment of GFP transduced SS-AF-MPCs. **(A)** GFP-SS-AF-MPCs were trapped in different tissues as evaluated by immunohistochemistry, 4 and 10 days after transplantation. GFP-SS-AF-MPCs were found in liver, spleen, lung and kidney at low frequency. Immunohistochemistry was performed by using anti-GFP antibody. Quantitation of GFP cells was determined by **(B)** FACS analysis and **(C)** RT-PCR in the respective tissues 4 or 10 days post-injection where percentage of positive cells and GFP fold expression difference is presented, respectively. As negative controls, non-injected mice were used. Values are shown as mean  $\pm$  S.D. for four mice in each group. **(D)** (i) Representative post-mortem fluorescent microscopy image of SS-AF-MPCs within the matrigel revealed a robust engraftment. (ii) FACS analysis of the disassociated matrigel area in presence of GFP transduced SS-AF-MPCs (red filled histogram) or GFP transduced SS-AF-MPCs in PBS (open histogram) 1 and 10 days post-transplantation.

1 from our group and others, yielded in an adherent heterogenic  
2 cell population with diverse morphology [7, 8, 11]. The  
3 expression analysis, determined by FACS analysis, documented  
4 the presence of CD44, CD90, CD73 and CD105 and the  
5 absence of haematopoietic-related CD-antigens [7, 8, 11],  
6 resembling to the phenotype of MSC-like cells according to  
7 standard criteria [43].

8 In our previous studies, we successfully isolated and expanded  
9 karyotypically normal MSCs from 80 samples of second trimester  
10 AF and performed a systematic phenotypic, molecular and pro-  
11 teomic analysis [7]. The main characteristic of the AF-MSCs was  
12 the high number of isolated cells and their rapid expansion *in vitro*  
13 compared to BM-MSCs. More importantly, these cells when  
14 exposed to appropriate differentiation media *in vitro*, showed a  
15 multilineage differentiation potential and ability to overcome the  
16 mesodermal commitment, by differentiating into cell types derived  
17 from all three germ layers [7].

18 In this study, we focused on the detailed investigation of differ-  
19 ent populations of AF-MPCs. We initially observed that unselected  
20 cultures contained, at passage 0–1, two morphologically distinct  
21 populations, SS-AF-MPCs and RS-AF-MPCs, whereas at passage  
22 2–3 the RS cells were more abundant in 94% of the samples. The  
23 rest 6% of the samples represented a SS cell population that can  
24 be expanded up to 40–50 passages to date. In an attempt to char-  
25 acterize better these two subpopulations, we randomly chose six  
26 AF samples at passage 0, where a mixture of both cell types  
27 existed at almost equal frequency, then we mechanically isolated  
28 SS or RS colonies and successfully expanded them under the  
29 same culture conditions.

30 Although cultures of MPCs have been studied extensively the  
31 last decades, standard criteria for isolating and expanding these  
32 cells have not been developed [4]. Several protocols have been  
33 established for isolating human MPCs from different sources by  
34 using staining with different antibodies [3, 4, 6–9, 11, 13, 16, 44].  
35 Other groups have reported that the existence of morphologically  
36 distinct MPC subpopulations is related to the plating density of the  
37 sample [1, 4, 44]. However, in this study, we observed the pres-  
38 ence of both RS-AF-MPCs and SS-AF-MPCs at passage 0 despite  
39 the initial plating density.

40 A detailed examination of the phenotype of SS-AF-MPCs and  
41 RS-AF-MPCs showed that SS-AF-MPCs expressed higher levels  
42 of CD90. However, the unselected AF-MPCs cultures at passage  
43 0–1 exhibited a mixed expression of CD90 revealing the initial co-  
44 existence of both SS and RS cells. This observation was consistent  
45 with older reports on murine lung fibroblasts and UCB-MPCs, in  
46 which two morphologically different populations were identified,  
47 one SS and CD90 positive, and the other one rounded and CD90  
48 negative. Furthermore, it has been shown that CD90 expression  
49 affected the morphology, proliferation and differentiation of fibro-  
50 blasts [45]. RS-AF-MPCs shared similar morphological characteris-  
51 tics to human amniotic membrane epithelial cells (hAEC), which  
52 express stem cell markers and have the ability to differentiate to  
53 multiple cell lineages [46]. However, hAEC differentiate success-  
54 fully to hepatocytes and exhibit increased expression of CD90 after  
55

second passage in culture, in contrast to RS-AF-MPCs [46].  
In addition, SS-AF-MPCs shared the rapid expansion and the  
multi-lineage differentiation potential of human umbilical cord  
perivascular cells (HUCPVCs), whereas they exhibited low expres-  
sion of CD146, a marker characteristic for circulating endothelial  
cells [47].

We further decided to study in more detail the molecular  
identity and specific properties of the SS-AF-MPC population.  
We observed that CD90 expression was decreased when the  
proliferation rate of SS-AF-MPCs was reduced because of tem-  
perature change. These results showed that CD90 antigen  
expression could be related to the growth rate of AF-MPCs and  
may in turn explain the difference of proliferation between  
SS-AF-MPCs (CD90<sup>high</sup>) and RS-AF-MPCs (CD90<sup>low</sup>) subpopula-  
tions. However, temperature change may also affect other  
biological parameters and for this reason further investigation is  
needed to explore the signaling pathway that is possibly related  
to this observation.

Furthermore, despite the similar stem cell features of SS-AF-  
MPCs and RS-AF-MPCs, the first ones possess a significantly  
higher migration capacity, compared to RS-AF-MPCs. This find-  
ing provided a basis for a more extended investigation of the  
migration mechanism of SS-AF-MPCs, involving a variety of  
adhesion molecules such as VLA-4, VLA-5, CD29 or CD44 [48].  
For example, blocking studies by using CD44 neutralizing  
antibody showed impaired migration properties of SS-AF-MPCs  
on fibronectin.

SS-AF-MPCs and RS-AF-MPCs expressed the pluripotency  
markers Oct-4 and Sox-2, indicating a possible primitive pheno-  
type and stem cell potential of these cells. Similar findings by  
Guillot *et al.* [7, 49] for MSCs isolated from first-trimester foetal  
blood, liver and BM confirmed that MSCs derived from neonatal  
and mid-gestational foetal tissues also expressed pluripotency  
markers, such as Oct-4 and Sox-2. In parallel, comparative  
studies by Greco *et al.* [50], showed that MSCs and embryonic  
stem cells (ESCs) shared similar expression of the embryonic  
transcription factors Oct-4, Sox-2 and Nanog, both at RNA and  
protein levels.

In addition, by the use of proteomic analysis, 25 proteins were  
found differentially expressed among the two subpopulations,  
which might explain the discrepancy in their proliferation, migration  
and differentiation properties. The differentially expressed proteins  
between SS-AF-MPCs and RS-AF-MPCs did not include any of the  
proteins highly expressed in MSCs from various sources such as  
Vimentin, Galectin, Gelsolin and Prohibitin [7, 47].

Our data indicated for the first time that SS-AF-MPCs are  
highly susceptible to lentiviral transduction, with no silencing  
effects over the multiple culture passaging. Moreover, GFP  
expression was retained through *in vitro* differentiation of SS-  
AF-MPCs, indicating the prospective utilization of this type of  
MPCs in gene therapy applications. Previous studies showed  
that human AF stem cells, seeded in a scaffold and exposed to  
osteogenic-inducing medium, can form bone *in vivo* [9].  
However, up to date there have been no conclusive reports

1 demonstrating the *in vivo* contribution of AF-MPCs upon  
2 intravenous delivery without tissue damage of the recipient  
3 animals. Here, we report that the SS-AF-MPCs can home into  
4 several tissues, at low frequency, after systemic infusion into  
5 recipient animals and can be tracked in lung, liver or spleen after  
6 several days. More importantly, we have demonstrated that  
7 matrigel supported SS-AF-MPCs engraftment is superior to cells  
8 alone. This can be explained by the specific properties of the  
9 matrigel basement, providing growth factors and structural  
10 support to the cells [6, 45, 51–53].

11 Therefore, we succeeded in mechanically isolating and  
12 expanding two mesenchymal origin populations of AF (SS-AF-  
13 MPCs and RS-AF-MPCs) that co-exist at early passage. SS-AF-  
14 MPCs are characterized by higher CD90 antigen expression  
15 than RS-AF-MPCs. The ease with which SS-AF-MPCs can be  
16 expanded in culture represents a marked contrast to the diffi-  
17 culties that have been encountered in expanding MPCs derived  
18 from sources such as BM, AF or UCB [6, 7, 9, 11, 31]. The  
19 specific properties of SS-AF-MPCs related to migration ability,  
20 differentiation capacity, lentiviral transduction efficiency and  
21 long-term survival *in vivo* will be of great importance in their  
22 use for cell and gene therapy. Under the conditions developed  
23 in this study, from a 10 ml AF sample we can mechanically  
24 isolate SS-AF-MPCs colonies that can generate millions of cells  
25 in culture in a short period of time, enough for future clinical  
26 applications.

## 30 Acknowledgements

31 This research was supported by Grant PENED No. 03ED 652 from the  
32 Greek Secretariat of Research and Technology and the European Union to  
33 N.P.A. Partial support was provided by Iaso Hospital, Athens, Greece. We  
34 would like to thank Professor Luigi Naldini for the generous donation of the  
35 pCCLsin.PPT.hPGK.GFP plasmid. We would like also to thank K. Vougas  
36 for his help on the proteomic analysis. Finally, we would like to thank  
37 Professor Thalia Papayannopoulou for her scientific advices and critical  
38 review of the paper.

## 41 References

- 44 1. **Smith JR, Pochampally R, Perry A, et al.** Isolation of a highly clonogenic and multi-  
45 potential subfraction of adult stem cells  
46 from bone marrow stroma. *Stem Cells*.  
47 2004; 22: 823–31.
- 48 2. **Sekiya I, Larson BL, Smith JR, et al.**  
49 Expansion of human adult stem cells from  
50 bone marrow stroma: conditions that max-  
51 imize the yields of early progenitors and  
52 evaluate their quality. *Stem Cells*. 2002;  
53 20: 530–41.
- 54 3. **Prockop DJ, Sekiya I, Colter DC.** Isolation  
55 and characterization of rapidly self-renewing  
stem cells from cultures of human marrow  
stromal cells. *Cytotherapy*. 2001; 3:  
393–6.
4. **Colter DC, Sekiya I, Prockop DJ.**  
Identification of a subpopulation of rapidly  
self-renewing and multipotential adult  
stem cells in colonies of human marrow  
stromal cells. *Proc Natl Acad Sci U S A*.  
2001; 98: 7841–5.
5. **Lee RH, Hsu SC, Munoz J, et al.** A subset  
of human rapidly self-renewing marrow  
stromal cells preferentially engraft in mice.  
*Blood*. 2006; 107: 2153–61.
6. **Chang YJ, Tseng CP, Hsu LF, et al.**  
Characterization of two populations of  
mesenchymal progenitor cells in umbilical  
cord blood. *Cell Biol Int*. 2006; 30:  
495–9.
7. **Roubelakis MG, Pappa KI, Bitsika V,  
et al.** Molecular and proteomic character-  
ization of human mesenchymal stem cells  
derived from amniotic fluid: comparison to  
bone marrow mesenchymal stem cells.  
*Stem Cells Dev*. 2007; 16: 931–52.
8. **In 't Anker PS, Noort WA, Scherjon SA,  
et al.** Mesenchymal stem cells in human

## Conflict of interest

The authors confirm that there are no conflicts of interest.

## Supporting information

Additional Supporting Information may be found in the online ver-  
sion of this article:

**Fig. S1 (A)** Immunofluorescent nuclear staining for E-cadherin, N-  
cadherin and Vimentin proteins merged with DAPI staining of SS-  
and RS- AF-MPCs. Original magnifications, 40×. **(B)** Comparative  
analysis of the percentage of proliferation of SS-AF-MPCs (blue line)  
and GFP-SS-AF-MPCs (red line) during 7 days of culture. **(C)** GFP  
transduced SS-AF-MPCs differentiation to adipocyte, osteocytes and  
hepatocytes. **(D)** Representative FACS histograms of SS-AF-MPCs  
(black filled histograms) and mouse BM-MSCs (grey filled histo-  
grams) gated for CD90, prior to analysis with the isotype-matched  
negative controls (blue and red open histograms), respectively. **(E)**  
Normal karyotype of (i) SS-AF-MPCs and (ii) RS-AF-MPCs from two  
representative samples derived from male [46XY(20)] and female  
embryo [46XX(20)], respectively at passage 5. (iii) Normal karyotype  
of SS-AF-MPCs from 1 representative sample derived from female  
embryo [46XX(20)], at passage 32. Forty metaphase spreads were  
fully analysed and karyotyped in each case.

**Table S1** Proteins up-regulated in SS-AF-MPCs

**Table S2** Proteins up-regulated in RS-AF-MPCs

**Table S3** Proteins expressed in RS-AF-MPCs only

Please note: Wiley-Blackwell is not responsible for the content or  
functionality of any supporting information supplied by the  
authors. Any queries (other than missing material) should be  
directed to the corresponding author for the article.

- 1 second-trimester bone marrow, liver, lung,  
2 and spleen exhibit a similar immunophe-  
3 notype but a heterogeneous multilineage  
4 differentiation potential. *Haematologica*.  
5 2003; 88: 845–52.
- 6 9. **De Coppi P, Bartsch G Jr, Siddiqui MM,**  
7 **et al.** Isolation of amniotic stem cell lines  
8 with potential for therapy. *Nat Biotechnol*.  
9 2007; 25: 100–6.
- 10 10. **In 't Anker PS, Scherjon SA, Kleijburg-**  
11 **van der Keur C, et al.** Amniotic fluid as a  
12 novel source of mesenchymal stem cells  
13 for therapeutic transplantation. *Blood*.  
14 2003; 102: 1548–9.
- 15 11. **Tsai MS, Lee JL, Chang YJ, et al.**  
16 Isolation of human multipotent mesenchy-  
17 mal stem cells from second-trimester  
18 amniotic fluid using a novel two-stage cul-  
19 ture protocol. *Hum Reprod*. 2004; 19:  
20 1450–6.
- 21 12. **Tsai MS, Hwang SM, Tsai YL, et al.**  
22 Clonal amniotic fluid-derived stem cells  
23 express characteristics of both mesenchy-  
24 mal and neural stem cells. *Biol Reprod*.  
25 2006; 74: 545–51.
- 26 13. **Prusa AR, Hengstschlager M.** Amniotic  
27 fluid cells and human stem cell research: a  
28 new connection. *Med Sci Monit*. 2002; 8:  
29 RA253–7.
- 30 14. **Hoehn H, Salk D.** Morphological and bio-  
31 chemical heterogeneity of amniotic fluid  
32 cells in culture. *Methods Cell Biol*. 1982;  
33 26: 11–34.
- 34 15. **Gosden CM.** Amniotic fluid cell types and  
35 culture. *Br Med Bull*. 1983; 39: 348–54.
- 36 16. **Fauza D.** Amniotic fluid and placental stem  
37 cells. *Best Pract Res Clin Obstet Gynaecol*.  
38 2004; 18: 877–91.
- 39 17. **Meirelles Lda S, Nardi NB.** Murine  
40 marrow-derived mesenchymal stem cell:  
41 isolation, in vitro expansion, and charac-  
42 terization. *Br J Haematol*. 2003; 123:  
43 702–11.
- 44 18. **Zhu H, Mitsuhashi N, Klein A, et al.** The  
45 role of the hyaluronan receptor CD44 in  
46 mesenchymal stem cell migration in the  
47 extracellular matrix. *Stem Cells*. 2006; 24:  
48 928–35.
- 49 19. **Yang MC, Chi NH, Chou NK, et al.** The  
50 influence of rat mesenchymal stem cell  
51 CD44 surface markers on cell growth,  
52 fibronectin expression, and cardiomyo-  
53 genic differentiation on silk fibroin –  
54 Hyaluronic acid cardiac patches. *Biomaterials*.  
55 2009; 31: 854–62.
20. **Grisafi D, Piccoli M, Pozzobon M, et al.**  
High transduction efficiency of human  
amniotic fluid stem cells mediated by ade-  
novirus vectors. *Stem Cells Dev*. 2008; 17:  
953–62.
21. **Boker W, Yin Z, Drosse I, et al.** Intro-  
ducing a single-cell-derived human  
mesenchymal stem cell line expressing  
hTERT after lentiviral gene transfer. *J Cell  
Mol Med*. 2008; 12: 1347–59.
22. **Meyerrose TE, Roberts M, Ohlemiller  
KK, et al.** Lentiviral-transduced human  
mesenchymal stem cells persistently  
express therapeutic levels of enzyme in a  
xenotransplantation model of human dis-  
ease. *Stem Cells*. 2008; 26: 1713–22.
23. **Piersanti S, Sacchetti B, Funari A, et al.**  
Lentiviral transduction of human postnatal  
skeletal (stromal, mesenchymal) stem  
cells: in vivo transplantation and gene  
silencing. *Calcif Tissue Int*. 2006; 78:  
372–84.
24. **Leschot NJ, Verjaal M, Treffers PE.** Risks  
of midtrimester amniocentesis; assess-  
ment in 3000 pregnancies. *Br J Obstet  
Gynaecol*. 1985; 92: 804–7.
25. **Eddleman KA, Malone FD, Sullivan  
L, et al.** Pregnancy loss rates after  
midtrimester amniocentesis. *Obstet Gynecol*.  
2006; 108: 1067–72.
26. **Buhring HJ, Battula VL, Tremi S, et al.**  
Novel markers for the prospective isolation  
of human MSC. *Ann N Y Acad Sci*. 2007;  
1106: 262–71.
27. **Zannettino AC, Roubelakis M, Welldon  
KJ, et al.** Novel mesenchymal and  
haematopoietic cell isoforms of the SHP-2  
docking receptor, PZR: identification,  
molecular cloning and effects on cell  
migration. *Biochem J*. 2003; 370: 537–49.
28. **Dull T, Zufferey R, Kelly M, et al.** A third-  
generation lentivirus vector with a condi-  
tional packaging system. *J Virol*. 1998;  
72: 8463–71.
29. **Siapati EK, Bigger BW, Miskin J, et al.**  
Comparison of HIV- and EIAV-based  
vectors on their efficiency in transducing  
murine and human hematopoietic  
repopulating cells. *Mol Ther*. 2005; 12:  
537–46.
30. **Goodwin HS, Bicknese AR, Chien SN,  
et al.** Multilineage differentiation activity  
by cells isolated from umbilical cord blood:  
expression of bone, fat, and neural mark-  
ers. *Biol Blood Marrow Transplant*. 2001;  
7: 581–8.
31. **Pittenger MF, Mackay AM, Beck SC,  
et al.** Multilineage potential of adult  
human mesenchymal stem cells. *Science*.  
1999; 284: 143–7.
32. **Jensen PK, Therkelsen AJ.** Cultivation at  
low temperature as a measure to prevent  
contamination with fibroblasts in epithelial  
cultures from human skin. *J Invest  
Dermatol*. 1981; 77: 210–2.
33. **Maier KG, Sadowitz B, Cullen S,  
et al.** Thrombospondin-1-induced vascular  
smooth muscle cell migration is dependent  
on the hyaluronic acid receptor CD44. *Am  
J Surg*. 2009; 198: 664–9.
34. **Niwa H, Miyazaki J, Smith AG.** Quan-  
titative expression of Oct-3/4 defines  
differentiation, dedifferentiation or self-  
renewal of ES cells. *Nat Genet*. 2000; 24:  
372–6.
35. **Trosko JE.** From adult stem cells to cancer  
stem cells: Oct-4 Gene, cell-cell communi-  
cation, and hormones during tumor pro-  
motion. *Ann N Y Acad Sci*. 2006; 1089:  
36–58.
36. **Huang CH, Chen MH, Young TH, et al.**  
Interactive effects of mechanical stretching  
and extracellular matrix proteins on initiat-  
ing osteogenic differentiation of human  
mesenchymal stem cells. *J Cell Biochem*.  
2009; 108: 1263–73.
37. **Abramovici H, Mojtabaie P, Parks RJ,  
et al.** Diacylglycerol kinase zeta regulates  
actin cytoskeleton reorganization through  
dissociation of Rac1 from RhoGDI. *Mol  
Biol Cell*. 2009; 20: 2049–59.
38. **Ivakhno SS, Kornelyuk AI.** Cytokine-like  
activities of some aminoacyl-tRNA syn-  
thetases and auxiliary p43 cofactor of  
aminoacylation reaction and their role in  
oncogenesis. *Exp Oncol*. 2004; 26:  
250–5.
39. **Tung JJ, Hobert O, Berryman M, et al.**  
Chloride intracellular channel 4 is involved  
in endothelial proliferation and morpho-  
genesis in vitro. *Angiogenesis*. 2009; 12:  
209–20.
40. **Davidson SM, Morange M.** Hsp25 and the  
p38 MAPK pathway are involved in differ-  
entiation of cardiomyocytes. *Dev Biol*.  
2000; 218: 146–60.
41. **Park SH, Cho HN, Lee SJ, et al.** Hsp25-  
induced radioresistance is associated with  
reduction of death by apoptosis: involve-  
ment of Bcl2 and the cell cycle. *Radiat Res*.  
2000; 154: 421–8.
42. **Anjos-Afonso F, Siapati EK, Bonnet D.** In  
vivo contribution of murine mesenchymal  
stem cells into multiple cell-types under  
minimal damage conditions. *J Cell Sci*.  
2004; 117: 5655–64.
43. **Dominici M, Le Blanc K, Mueller I, et al.**  
Minimal criteria for defining multipotent  
mesenchymal stromal cells. The  
International Society for Cellular Therapy  
position statement. *Cytotherapy*. 2006; 8:  
315–7.
44. **Colter DC, Class R, DiGirolamo CM,  
et al.** Rapid expansion of recycling stem  
cells in cultures of plastic-adherent cells

- 1 from human bone marrow. *Proc Natl Acad*  
2 *Sci U S A.* 2000; 97: 3213–8.
- 3 45. **Rege TA, Hagood JS.** Thy-1 as a regulator  
4 of cell-cell and cell-matrix interactions in  
5 axon regeneration, apoptosis, adhesion,  
6 migration, cancer, and fibrosis. *FASEB J.*  
7 2006; 20: 1045–54.
- 8 46. **Parolini O, Alviano F, Bagnara GP, et al.**  
9 Concise review: isolation and characteriza-  
10 tion of cells from human term placenta: out-  
11 come of the first international Workshop on  
12 Placenta Derived Stem Cells. *Stem Cells.*  
13 2008; 26: 300–11.
- 14 47. **Sarugaser R, Lickorish D, Baksh D,**  
15 **et al.** Human umbilical cord perivascular  
16 (HUCPV) cells: a source of mesenchymal  
17 progenitors. *Stem Cells.* 2005; 23:  
18 220–9.
- 19 48. **Mostafavi-Pour Z, Askari JA, Parkinson**  
20 **SJ, et al.** Integrin-specific signaling path-  
21 ways controlling focal adhesion formation  
22 and cell migration. *J Cell Biol.* 2003; 161:  
23 155–67.
- 24 49. **Guillot PV, Gotherstrom C, Chan J,**  
25 **et al.** Human first-trimester fetal MSC  
26 express pluripotency markers and grow  
27 faster and have longer telomeres than  
28 adult MSC. *Stem Cells.* 2007; 25:  
29 646–54.
- 30 50. **Greco SJ, Liu K, Rameshwar P.** Functional  
31 similarities among genes regulated  
32 by OCT4 in human mesenchymal and  
33 embryonic stem cells. *Stem Cells.* 2007; 25:  
34 3143–54.
- 35 51. **Bieback K, Kern S, Kluter H, et al.** Critical  
36 parameters for the isolation of mesenchy-  
37 mal stem cells from umbilical cord blood.  
38 *Stem Cells.* 2004; 22: 625–34.
- 39 52. **Erices A, Conget P, Minguell JJ.**  
40 Mesenchymal progenitor cells in human  
41 umbilical cord blood. *Br J Haematol.* 2000;  
42 109: 235–42.
- 43 53. **Phipps RP, Penney DP, Keng P, et al.**  
44 Characterization of two major populations  
45 of lung fibroblasts: distinguishing mor-  
46 phology and discordant display of Thy 1  
47 and class II MHC. *Am J Respir Cell Mol*  
48 *Biol.* 1989; 1: 65–74.

**Author Queries**

Q1 Author: A colour work agreement form (CWA) has not been received for this article. A completed CWA is necessary for reproduction of coloured figures. Please download the form from [http://onlinelibrary.wiley.com/journal/10.1111/\(ISSN\)1582-4934/homepage/JCMM\\_CWA\\_2010.pdf](http://onlinelibrary.wiley.com/journal/10.1111/(ISSN)1582-4934/homepage/JCMM_CWA_2010.pdf) and return it along with your corrections to the Production Editor.